

JGR Biogeosciences

RESEARCH ARTICLE

10.1029/2023JG007514

Special Section:

Fjords: Estuaries on the Front-line of Climate Change

Key Points:

- Glacier-derived particles release 2–46% of labile particulate lead (Pb) upon mixing with seawater
- Pb dynamics in glacier fjords are characterized by a rapid release of dissolved Pb followed by readsorption on a timescale of hours-to-days
- Dissolved Pb release from the Greenland Ice Sheet is likely within the range 0.2–1 Mmol yr⁻¹

Supporting Information:

Supporting Information may be found in the online version of this article.

Correspondence to:

M. J. Hopwood,
mark@sustech.edu.cn

Citation:

Krause, J., Zhu, X., Höfer, J., Achterberg, E. P., Engel, A., Meire, L., et al. (2023). Glacier-derived particles as a regional control on marine dissolved Pb concentrations. *Journal of Geophysical Research: Biogeosciences*, 128, e2023JG007514. <https://doi.org/10.1029/2023JG007514>

Received 13 APR 2023

Accepted 20 SEP 2023

Author Contributions:

Conceptualization: Jana Krause, Juan Höfer, Lorenz Meire, Mark J. Hopwood

Data curation: Jana Krause

Formal analysis: Jana Krause, Xunchi Zhu, Alice E. Stuart-Lee, Mark J. Hopwood







Funding acquisition: Eric P. Achterberg, Anja Engel, Mark J. Hopwood

Investigation: Jana Krause, Xunchi Zhu, Juan Höfer, Lorenz Meire, Alice E. Stuart-Lee, Mark J. Hopwood

Methodology: Eric P. Achterberg, Anja Engel, Mark J. Hopwood

Project Administration: Juan Höfer, Mark J. Hopwood

Glacier-Derived Particles as a Regional Control on Marine Dissolved Pb Concentrations

Jana Krause¹, Xunchi Zhu^{1,2}, Juan Höfer^{3,4} , Eric P. Achterberg¹ , Anja Engel¹ , Lorenz Meire^{5,6} , Alice E. Stuart-Lee⁵ , and Mark J. Hopwood² 

¹Marine Biogeochemistry, GEOMAR Helmholtz Centre for Ocean Research Kiel, Kiel, Germany, ²Department of Ocean Science and Engineering, Southern University of Science and Technology, Shenzhen, China, ³Escuela de Ciencias del Mar, Pontificia Universidad Católica de Valparaíso, Valparaíso, Chile, ⁴Centro FONDAP de Investigación en Dinámica de Ecosistemas Marinos de Altas Latitudes (IDEAL), Valdivia, Chile, ⁵Department of Estuarine and Delta Systems, Royal Netherlands Institute for Sea Research, Yerseke, The Netherlands, ⁶Greenland Climate Research Centre, Greenland Institute of Natural Resources, Nuuk, Greenland

Abstract Higher than expected concentrations of dissolved lead (dPb) have been consistently observed along glaciated coastlines and it is widely hypothesized that there is a net release of dPb from glacier-derived sediments. Here we further corroborate that dPb concentrations in diverse locations around west Greenland (3.2–252 pM) and the Western Antarctic Peninsula (7.7–107 pM) appear to be generally higher than can be explained by addition of dPb from glacier-derived freshwater. The distribution of dPb across the salinity gradient is unlike any other commonly studied trace element (e.g., Fe, Co, Ni, Cu, Mn, and Al) implying a dynamic, reversible exchange between dissolved and labile particulate Pb. Incubating a selection of glacier-derived particles from SW Greenland (Ameralik and Nuup Kangerlua) and Svalbard (Kongsfjorden), with a range of labile particulate Pb (LpPb) content (11–113 nmol g⁻¹), the equivalent of 2–46% LpPb was released as dPb within 24 hr of addition to Atlantic seawater. Over longer time periods, the majority of this dPb was typically readsorbed. Sediment loading was the dominant factor influencing the net release of dPb into seawater, with a pronounced decline in net dPb release efficiency when sediment load increased from 20 to 500 mg L⁻¹. Yet temperature also had some effect with 68 ± 22% higher dPb release at 11°C compared to 4°C. Future regional changes in dPb dynamics may therefore be more sensitive to short-term suspended sediment dynamics, and potentially temperature changes, than to changing interannual runoff volume.

Plain Language Summary Glacier runoff is a minor source of the element lead (Pb) into the ocean. Lead that was deposited on ice surfaces from atmospheric deposition is ultimately released in runoff and drains into the ocean. Changes in the concentration of Pb in fresh and marine waters are of concern because Pb is a toxic element with the potential to have detrimental effects on ecosystems and public health. Across most of the Atlantic and Arctic, Pb concentrations have been strongly affected by the historical use of Pb as a fuel additive. This led to elevated atmospheric deposition of Pb until the 1990s when these additives were extensively phased out. Around glaciated coastlines however, evidence is emerging worldwide of a natural Pb source too large to be explained by atmospheric deposition. This source is thought to be related to the release of Pb from glacier erosion. Here we corroborate these observations in southwestern Greenland and the Western Antarctic Peninsula showing that a dynamic release and readsorption of Pb from glacier-derived particles explains the observed distribution of dissolved Pb in seawater.

1. Introduction

Around the periphery of the Arctic and Antarctic, glaciers, icebergs, and freshwater runoff deliver high loads of lithogenic particles (Azetsu-Scott & Syvitski, 1999; Overeem et al., 2017; Shaw et al., 2011) and elevated concentrations of some dissolved trace metals including iron (Fe), manganese (Mn), copper (Cu), cobalt (Co), nickel (Ni), lead (Pb), and aluminum (Al) into the coastal ocean (Annett et al., 2015; Brown et al., 2010; Forsch et al., 2021; Krause et al., 2021; Krisch et al., 2021; Schlosser & Garbe-Schönberg, 2019). The extent to which glacier-derived particles act as sources or sinks of individual trace elements in the coastal ocean depends upon numerous physical and biogeochemical factors including the lability, sinking rate, and burial rates of particles, the extent to which different trace elements tend to be scavenged from solution and the nature of benthic processes (Forsch et al., 2021; Herbert et al., 2020; Merwe et al., 2019). Iron is for example, characterized by a rapid and

Resources: Juan Höfer, Eric P. Achterberg, Anja Engel
Supervision: Eric P. Achterberg, Anja Engel, Lorenz Meire, Mark J. Hopwood
Visualization: Juan Höfer
Writing – original draft: Jana Krause, Mark J. Hopwood
Writing – review & editing: Jana Krause, Xunchi Zhu, Juan Höfer, Anja Engel, Lorenz Meire, Alice E. Stuart-Lee, Mark J. Hopwood

pronounced transfer of dissolved (<0.2 μm) phases onto particle surfaces following glacier discharge into the ocean, with $\sim 98\%$ of dissolved Fe removed at intermediate salinities, mainly due to aggregation of inorganic colloids (Kanna et al., 2020; Schroth et al., 2014; Zhang et al., 2015). Other dissolved trace metals including Co, Ni, Cu, Mn, and Al behave more conservatively across the salinity gradient suggesting either a more limited and/or balanced exchange between labile particulate and dissolved phases (Brown et al., 2010; Krause et al., 2021; Michael et al., 2023). Dissolved Pb in these environments may however exhibit a unique behavior due to the dynamic exchange typically observed between dissolved Pb (dPb) and labile particulate Pb phases (Noble et al., 2015; Rusiecka et al., 2018; Sherrell et al., 1992). To date however there are few data sets available to characterize the underlying mechanism and thus assess how marine dPb concentrations in glaciated regions may change as a result of future glacier retreat or increases in glacial discharge.

Elevated concentrations of Pb in some Arctic terrestrial environments, including the cryosphere, are associated with a legacy of anthropogenic contamination from increased atmospheric deposition since the industrial revolution (Boyle et al., 1994; Candelone et al., 1995; Łokas et al., 2016). Anthropogenic derived Pb is certainly a contributing factor to Pb distributions in the Arctic (Bazzano et al., 2017; Boyle et al., 1994; Hong et al., 1994). Yet dPb distributions and $^{206}\text{Pb}/^{207}\text{Pb}$ and $^{208}\text{Pb}/^{207}\text{Pb}$ isotopic ratios in both glaciated Arctic and Antarctic locations suggest the existence of a sediment associated dPb source which is primarily nonanthropogenic in origin. Higher than expected dPb concentrations of up to 46 pM in Cumberland Bay (South Georgia) suggest a source of dPb associated with particles in the bay (Schlosser & Garbe-Schönberg, 2019) which is characterized by high turbidity from runoff (Schlosser et al., 2018). Similarly, based on its isotopic composition, a mineral source of dPb has been suggested to account for 95% of the 4–89 pM dPb observed close to the Dotson Ice Shelf (Antarctica) (Ndungu et al., 2016). Dissolved Pb concentrations of 30–120 pM in one survey of Maxwell Bay (King George Island) were also noted to be higher than could be explained by dilution of dPb in freshwater sources (Kim et al., 2015) and dPb concentrations of 12 pM emerging from beneath the floating ice tongue of Nioghalvfjærdsbræ (NE Greenland) suggest a twofold to threefold enrichment of dPb compared to concentrations in inflowing Atlantic water (Krisch et al., 2022). Similarly, near-surface dPb concentrations reported at two stations close to Devon Island (Canadian Arctic Archipelago) of 10.4 and 10.8 pM were elevated compared to both adjacent stations and values expected from conservative mixing of dPb concentrations (Colombo et al., 2019). Altogether, these studies consistently appear to show evidence of an additional dPb source at intermediate salinities across diverse glaciated regions worldwide (Colombo et al., 2019; Kim et al., 2015; Krisch et al., 2022; Ndungu et al., 2016; Schlosser & Garbe-Schönberg, 2019). There is also some evidence in the paleorecord to suggest elevated Pb deposition in the ocean associated with subglacial weathering (Crocket et al., 2013), however our mechanistic understanding of the effect of this process on marine dPb concentrations is limited.

Estuarine Pb dynamics in better studied temperate regions commonly show conservative dPb behavior, or nonconservative dPb loss (Abdel-Moati, 1990; Cenci & Martin, 2004; Elbaz-Poulichet et al., 1996), although these trends are not universal. Suspended particle loads may be a more important driver of dPb dynamics than salinity in estuarine systems (Benoit et al., 1994) confounding attempts to explain general dPb trends in terms of salinity alone. A key question is whether dPb dynamics differ between temperate rivers and high latitude glacier outflows. While we hypothesize that a desorption mechanism from glacier-derived particles may explain higher than expected dPb concentrations along glaciated coastlines (Schlosser & Garbe-Schönberg, 2019), a paucity of data across salinity gradients to characterize this, seasonal data to assess how net dPb release may change through the year in such localities, and incubation experiments to establish rates preclude the calculation of associated Pb fluxes. The residence time of any dPb released may also be highly dependent on local productivity levels, as uptake and adsorption to cell walls of dPb by plankton is thought to be a major sink for new additions of dPb to the ocean (Michaels & Flegal, 1990).

Glacier retreat worldwide is expected to continue this century irrespective of the Representative Concentration Pathways scenario that humanity tracks (IPCC Working Groups I & II, 2019). In the context of increasing discharge and exposure of proglacial sediments, it is clearly important to constrain any effects this may have on the mobility of toxic elements like Pb. It will be critical to assess the potential impacts on affected ecosystems (Cauvy-Fraunié & Dangles, 2019); the risks posed to water supplies (Fortner et al., 2011) and, given emerging interest in the subject, potentially also to evaluate the side effects of exploiting glacial rock flour as raw material for construction aggregates, agricultural, or enhanced weathering geoengineering applications (Bendixen et al., 2019; Pesch et al., 2021). Here we conduct a process study to investigate dPb dynamics across the salinity gradients in a series of glacier fjords in order to constrain the factors that may facilitate dPb release from glacier-derived particles and the fate of any dPb released. Field sites were selected because data for other dissolved trace elements is already

available from the same transects (in most cases for Fe, Co, Ni, Cu and Mn) (Krause et al., 2021; van Genuchten et al., 2022). Furthermore, in the case of SW and W Greenland, the geographic context with long, stratified fjords and steady gradients along the fjord surface, is favorable for investigating nonconservative processes which may be sensitive to shifts in key water properties such as turbidity, salinity or the distribution of primary producers. To address the possible influences of seasonality we include repeat sections of Nuup Kangerlua and Ameralik (SW Greenland) in boreal spring (May) and mid/late summer (August and September) 2019. This study focuses on inshore glaciated regions where multiple freshwater sources enter the ocean. Major freshwater sources include terrestrial runoff that enters the ocean at the surface and originates from ice melt or precipitation. Additionally, in regions with tidewater (marine-terminating) glaciers, freshwater enters the ocean from the submarine melting of ice at the glacier front, the melting of calved ice within fjords, and subglacial discharge entering the ocean at the glacier grounding line which originates from a combination of surface and basal melting processes. Additional minor sources of freshwater include submarine groundwater discharge, precipitation, and sea ice melt. Without specific tracers of different freshwater components, we cannot distinguish between these sources quantitatively, although some regional budgets (Bendtsen et al., 2015; Mortensen et al., 2011) and estimates for different source terms are available (Mankoff, Noël, et al., 2020; Mankoff, Solgaard, et al., 2020). By contrasting different fjords we can also gain some insight into the significance of different source terms, for example, by comparing the biogeochemistry of Nuup Kangerlua which hosts both land-terminating and marine-terminating glaciers (Juul-Pedersen et al., 2015) with the smaller, adjacent Ameralik which hosts only a land-terminating glacier system (Stuart-Lee et al., 2021).

2. Materials and Methods

2.1. Trace Metal Sampling and Analysis

Along-fjord transects were conducted in both Antarctica and Greenland (Figure 1) with methods for collection of trace metal clean samples on these field campaigns described previously (Krause et al., 2021). Briefly, fjord transects in W Greenland and spring cruises in SW Greenland on RV Sanna (Figure 1) used a towfish system mounted on a winch and deployed at ~1 m depth and ~2 m away from the ship when underway. Water was pumped continuously through plastic tubing which was precleaned with 0.1 M HCl (reagent grade), with suction provided by a Teflon diaphragm pump (Dellmeco, Germany, DM15). This continuous seawater supply was sampled inside a laminar flow hood. In other fjords, sampling from small rigid inflatable vessels was conducted from surface waters using acid cleaned 1 L high-density polyethylene bottles (Nalgene) deployed upwind of the boat, which were rinsed once and then filled and subsampled.

Trace metal clean low-density polyethylene (LDPE, Nalgene) bottles were prepared via a three-stage washing procedure (1 day in Mucosol detergent, 1 week in reagent grade 1.2 M HCl, and 1 week in reagent grade 1.2 M HNO₃) and then stored empty and double bagged in LDPE bags until use. Dissolved trace element samples were syringe filtered (0.2 μm, polyvinyl difluoride, Millipore), or filtered inline from the towfish system (AcroPak, polyethersulfone, 0.8/0.2 μm), into trace metal clean 125 mL LDPE bottles. Samples were then acidified to pH 1.9 by the addition of concentrated HCl (180 μL, UpA grade, Romil) within 1 day of sample collection and stored for >6 months prior to analysis. Samples were preconcentrated offline using a seaFAST (ESI) preconcentration system and analyzed via high resolution inductively coupled plasma mass spectrometry (HR-ICP-MS; ThermoFischer Element XR) exactly as per Rapp et al. (2017) with calibration via standard addition for Pb. Analysis was conducted on the same sample aliquots as prior work describing other trace metal concentrations (Fe, Co, Ni, Cu, and Mn; Krause et al., 2021; van Genuchten et al., 2022). To verify the accuracy of dPb measurements, reference materials were analyzed alongside samples; GSC measured 39 ± 2 pM (*n* = 14, consensus 39 ± 4 pM), GSP measured 82 ± 19 pM (*n* = 5, consensus 62 ± 5 pM), NASS-7 measured 10 ± 1 pM (*n* = 15, certified 13 ± 4 pM), CASS-6 measured 51 ± 7 pM (*n* = 18, certified 51 ± 19 pM). The combined field (deionized water treated as a sample) and seaFAST manifold blank was consistently low throughout all analysis (0.7 ± 1.7 pM dPb).

2.2. Macronutrients, CDOM, and Chlorophyll

Dissolved macronutrient concentrations (nitrate + nitrite, NO_x; phosphate, PO₄; and silicic acid, Si(OH)₄), also reported previously for transects discussed herein (Krause et al., 2021), were syringe filtered (0.2 μm, polyvinyl difluoride, Millipore) and stored refrigerated in the dark until analysis. Macronutrient concentrations were measured via a Quattro 39 System (SEAL) segmented flow analyzer with a XY2 Autosampler (Hansen & Koroleff, 1999). Detection limits, defined as three standard deviations of blank (deionized water) measurements, varied between

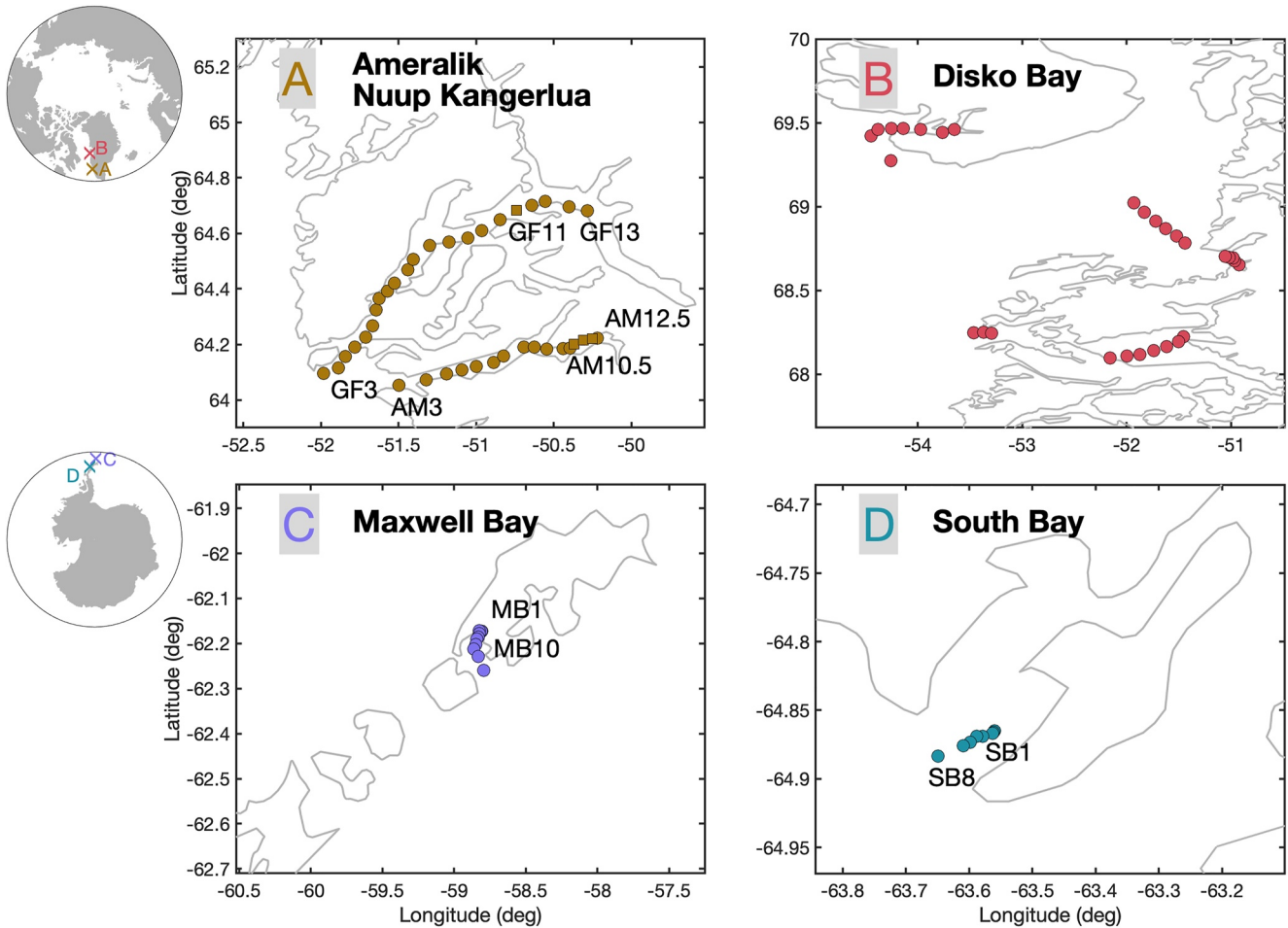


Figure 1. Field sites discussed within the text. Stations where surface water samples were collected (circles) within Ameralik (A), Nuup Kangerlua (A), Maxwell Bay (C), and South Bay (D). AM_x, GF_x, MB_x, and SB_x, respectively, refer to standard stations defined by the ongoing long-term monitoring projects Greenland Ecosystem Monitoring (GEM Database) and Centro de Investigación Dinámica de Ecosistemas Marinos de Altas Latitudes (IDEAL). For clarity, only the key stations are labeled. Nuup Kangerlua is also referred to in the literature as Godthåbsfjord. Suspended sediment was collected from sites AM10–12 and from ice collected in the vicinity of GF11 (squares in A).

batches yet were consistently $<0.10 \mu\text{M PO}_4$, $<0.10 \mu\text{M NO}_3$ and $<0.25 \mu\text{M Si(OH)}_4$ with precision (one standard deviation of triplicate samples) of 2.0%, 3.1%, and 0.5%, respectively. Si^* was calculated as $[\text{Si(OH)}_4] - [\text{NO}_x]$. Chlorophyll *a* (chl *a*) was determined the same day as sample collection after filtering 0.5 L of water onto GF/F filters (Whatman, $0.7 \mu\text{m}$) with subsequent extraction in 10 mL 90% acetone for 24 hr. Chlorophyll *a* fluorescence in the filtrate was then analyzed (TD-700, Turner Designs Trilogy laboratory fluorometer) before and after the addition of 200 μL 1 M HCl with calibration using a solid standard (Turner Designs). Tinted glass vials for chromophoric dissolved organic matter (CDOM) samples were cleaned with deionized water, then combusted in Al foil before use (450°C , >4 hr). CDOM samples were syringe filtered (CHROMAFIL Xtra, cellulose acetate, $0.2 \mu\text{m}$), after rinsing the filters and glass vials once, and then stored refrigerated. CDOM was analyzed within 3 months of sample collection using a Liquid Waveguide Capillary Cell (optical pathlength = 1.038 m) with a Micropack UV-VIS-NIR light source (DT-Mini2-GS) and an Ocean Optics USB4000 Spectrometer unit. The slope ratio (S_R , an indicator of molecular weight) was calculated as per Helms et al. (2008).

2.3. Physical Data

Where possible, sampling was coordinated to occur alongside CTD (conductivity, temperature, and depth) profiles. Salinity, temperature, and other parameters at 1 m depth are reported alongside trace metal data. When/where CTD profiles were not taken in close coordination with surface sampling, a handheld LF 325 conductivity

meter (WTW) was used to record in situ temperature and salinity. In Ameralik, suspended particle loads were determined by filtering 2 L bulk water samples onto precombusted and preweighed 25 mm GF/F filters (0.7 μm pore size) as reported by Stuart-Lee et al. (2023).

2.4. Particle Resuspension Experiments

To collect suspended particles for incubation experiments, unfiltered water was reserved in trace metal clean 1 L LDPE (Nalgene) bottles prepared as above. A vacuum pump with 0.2 μm polyethersulfone disk filters (47 mm diameter; Sartorius) was used to filter water aboard the ship immediately after sample collection. For each location, ~ 1 –2 L of fjord water was filtered (or less if the filter clogged). The disk filters with retained solids were then sealed in air-tight petri dishes while still wet and kept cold throughout the cruise (stored in -80°C freezer) and during shipment to the home institute (packed with ice). Samples described herein from Greenland are duplicate filters collected from a July 2015 campaign in Ameralik and Nuup Kangerlua (also known as Godthåbsfjord) described by van Genuchten et al. (2021) that is, multiple filters were collected and retained from the same sampling point. Sediment samples from Kongsfjorden (Svalbard) are also duplicates from a prior campaign in August 2016 (Hopwood et al., 2017) and were collected and stored similarly (at -20°C). A small quantity of core-top sediment from Kongsfjorden obtained from a bottom corer in June 2017 was also available (Laufer-Meiser et al., 2021). Herein we use six types of sediment/particle samples from Svalbard (glacier surface sediment, iceberg surface sediment, iceberg embedded sediment, proglacial stream sediment, suspended particles from Kongsfjorden surface water, and core-top sediment from the fjord) and two types of sediment/particle samples from SW Greenland (iceberg surface sediment, and suspended particles from Ameralik surface waters). Particle sizes were estimated using a Laser Particle Sizer (Analysette 22, Fritsch) after filtering through a 2 mm grid sieve. Core-top sediments from Svalbard and fjord suspended particles from Ameralik were not measured due to limited available quantities.

Labile particulate Pb (LpPb) for each sediment sample with sufficient mass available was determined following a 2 hr weak acid leach (Berger et al., 2008) (25% by volume acetic acid, Optima grade, Fisher Scientific) with a mild reducing agent (0.02 M hydroxylamine hydrochloride, Sigma TM grade) and a short heating step (10 min at 90 – 95°C). Analysis was via HR-ICP-MS as per dissolved metal samples. In all cases, to avoid the undesired effects of dewetting on mineral phases (Raiswell et al., 2010), sediment samples were used in incubations directly after defrosting. For most sediments, a wet slurry of $\sim 50\text{ g L}^{-1}$ was made and used to add wet sediment aliquots to incubation bottles. Separately, subsamples of the wet sediment were dried to constant mass at 60°C to determine sediment loads used in the incubations. For fjord suspended sediment (from Ameralik), due to low sediment quantities, the polyethersulfone disk filter was directly added to incubation experiments and similarly dry mass was determined on a filter fragment. Sediment loads of 20 – 500 mg L^{-1} (dry mass) were selected to mimic turbid inner-fjord surface environments where glacier-derived particles first enter the ocean (Overeem et al., 2017). Temperatures of 4°C or 11°C , and dark conditions or 2,500 lux light intensity, were selected for the same reason (based on summertime conditions in Nuup Kangerlua and Ameralik: van Genuchten et al., 2021; Meire et al., 2017; Stuart-Lee et al., 2021). All incubations were conducted in trace metal clean polycarbonate bottles (500 mL, Nalgene) using filtered (AcroPak, polyethersulfone, $0.8/0.2\ \mu\text{m}$) Atlantic seawater which had been stored for >1 year in the dark. Bottles were incubated in a temperature-controlled cabinet (MLR352, Panasonic) and manually shaken every few hours. Control bottles were incubated in parallel and contained only filtered seawater. Dark treatments were incubated wrapped in opaque black plastic in parallel with light treatments.

Two series of incubation experiments were conducted. In the first incubations, sediment was suspended in seawater for 24 hr in light or dark conditions with varying sediment loads from 20 to 500 mg L^{-1} . After 24 hr, incubation bottles were filtered (0.2 μm , PES, Sartorius) and dPb concentration determined. In the second incubations, multiple identical bottles were prepared for each treatment group. Sediment was suspended for up to 3 weeks in light or dark conditions with sediment load of either ~ 50 or 200 mg L^{-1} . At regular time intervals, one bottle from each treatment group was filtered and dPb concentration determined (the limited quantity of some sediment samples meant it was possible to conduct some incubations for longer time periods than others). Due to limited particle supply for the suspended Ameralik fjord samples, suspended particles from two CTD stations were used for the resuspension experiments, and suspended particles from an intermediate station were used to determine LpPb (total lateral distance between the stations $<10\text{ km}$, Figure 1). While there may be some changes in particle properties along the fjord due to progressive sedimentation, prior analysis of duplicate samples from the same transect, extending further away from the glacier than we consider herein, suggested minimal changes in mineralogy over this distance (van Genuchten et al., 2021).

2.5. Statistical Analysis of Transects

The relationships among summertime dPb concentrations, macronutrients, salinity, and lateral distance from the most terrestrially influenced point within each study region (determined from satellite imagery) were analyzed by means of a Redundancy Analysis (RDA). The RDA function (package *vegan*) within *R* version 4.0.2 was used to perform the RDA (Oksanen et al., 2020; R Core Team, 2012), while site scores were calculated as the weighted sum of species. RDA overall significance and the significance of RDA axes was assessed by a permutation test (10,000 iterations) using the *anova.cca* function (*vegan* package) to avoid the problems caused by nonnormal distributions (Borcard et al., 2011). For statistical analysis of transects it was necessary to interpolate some parameters onto the dPb distributions where measurements were made with some temporal or spatial offsets. Data was linearly interpolated by considering the position of stations along the transect. Nutrient and trace metal data were always obtained in parallel from the same sampled water; some chl *a* and turbidity data were interpolated. Trends in summertime dPb data were also assessed using Generalized Additive Models (Hastie & Tibshirani, 2014) which are advantageous for representing nonlinear effects such as the dynamic interaction between dPb and suspended particle load. GAMs were generated using the *gam* function from the *mgcv* package (Wood, 2011) as described previously for other trace elements (Krause et al., 2021).

3. Results

3.1. Dissolved Pb Distribution in Glacier Fjords

Concentrations of dPb were determined alongside other trace metals across four regions (Figure 1) at 131 stations. In two Antarctic coastal regions, median dPb was 23 pM with a range of 7.8–107 pM. Across five Greenlandic coastal regions the median dPb was 38 pM with a range of 3.2–252 pM (excludes one outlier of 1,246 pM). While there are sparse data sets to compare to, measured dPb concentrations fall within the range reported from similar geographic environments in the Arctic and Antarctic (Colombo et al., 2019; Kim et al., 2015; Krisch et al., 2022; Ndungu et al., 2016; Schlosser & Garbe-Schönberg, 2019). The February 2018 transect in Maxwell Bay (dPb concentrations 29–107 pM) is close to Marion Cove (3–6 km distance), both in King George Island, where similar concentrations were observed, 30–120 pM, in January 2012 (Kim et al., 2015).

For the Greenlandic catchments, all dPb concentrations >35 pM were observed in Nuup Kangerlua or the neighboring Ameralik. For Nuup Kangerlua these elevated dPb concentrations were not restricted to measurements in boreal summer (August/September) as moderately high dPb was also observed in boreal spring (May, ranges 19–251 pM Nuup Kangerlua, 6.5–12 pM Ameralik). Springtime data (May) were collected after the onset of the spring bloom (Juul-Pedersen et al., 2015) when freshwater flow entering these fjords is low compared to the annual maxima in July–August and largely consists of snow melt and ice melt (Mortensen et al., 2013; Mankoff, Noël, et al., 2020; Stuart-Lee et al., 2021) mid/late summertime (August and September) transects span the timing of the annual peak in meltwater discharge (Mankoff, Noël, et al., 2020). In Nuup Kangerlua, spring dPb concentrations of 67 ± 47 pM were similar to summertime concentrations of 77 ± 42 pM. In Ameralik, while the data set was smaller, the seasonal difference was more pronounced with dPb increasing from 9.1 ± 1.6 pM in May to 87 ± 86 pM in August (the difference increases further if one outlier dPb concentration from August is included).

For along-fjord transects of dPb there was no clear general trend for either an increase, or decrease in concentration with salinity (Figure 2). In only one individual Arctic transect a decline in dPb concentration with increasing salinity was observed (Nuuk Kangerlua, August 2019, $R^2 = 0.31$). In other fjords some slight increases of dPb with salinity were registered (Figure 2). Similarly, GAM fits for dPb considering salinity would be better described as being relatively constant across the salinity gradient, compared to other trace metals measured in these catchments to date (Krause et al., 2021). The dPb distribution was also profoundly different from macronutrients, and a redundancy analysis suggested weak relationships with turbidity and chl *a* (Figure 3). The best fitting GAM also included a general chlorophyll parameter that represented an increase in dPb with increasing chl *a* concentrations after removing the salinity effect (Figure 2).

3.2. General Biogeochemical Trends

Across the Greenlandic field sites, most biogeochemical parameters showed spatial trends which scale with salinity. The tracer Si* (calculated as $\text{Si}(\text{OH})_4 - \text{NO}_x$), which tracks the excess $\text{Si}(\text{OH})_4$ delivered by runoff into the ocean (Meire et al., 2016), is approximately linear across the salinity gradient (linear regression, $n = 96$, linear regression $R^2 = 0.66$ across all data for the five Greenlandic catchments herein). CDOM S_R , one indicator of

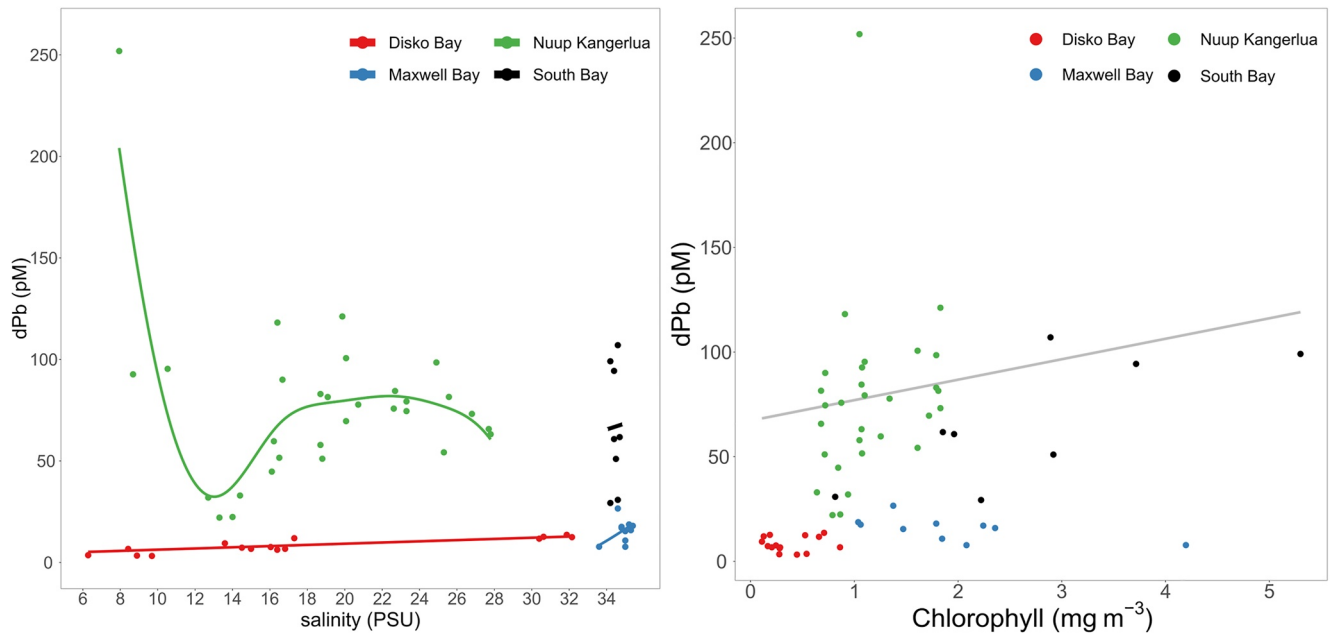


Figure 2. Summer dissolved lead (dPb) trends across catchments. (Left) GAM fits to the data considering a salinity effect (different for each catchment). Fits are shown for each catchment. (Right) GAM fits to the data considering a chlorophyll effect. For clarity, only the Nuup Kangerlua data—the most extensive—is plotted with a fit to show the effect. The points in both panels represent the actual data used to generate the best fitting GAM ($R^2 = 0.795$, (Salinity * Location) + Chl *a*).

changes in colored organic matter properties (Helms et al., 2008), is also approximately linear across the salinity gradient (linear regression, $n = 93$, $R^2 = 0.28$ across five Greenlandic catchments). Most trace metals (dFe, dCo, dNi, dCu, and dMn) showed a decline in concentration with increasing salinity (Krause et al., 2021), with dMn exhibiting the most conservative behavior, and dPb and dFe the least. These trends are generally less clear in the Antarctic field sites, but this may reflect lower and more diffusive freshwater inputs and thus less pronounced salinity gradients (observed salinity ranges were 33.6–35.4 for Maxwell Bay and 34.2–34.7 for South Bay, Figure 2).

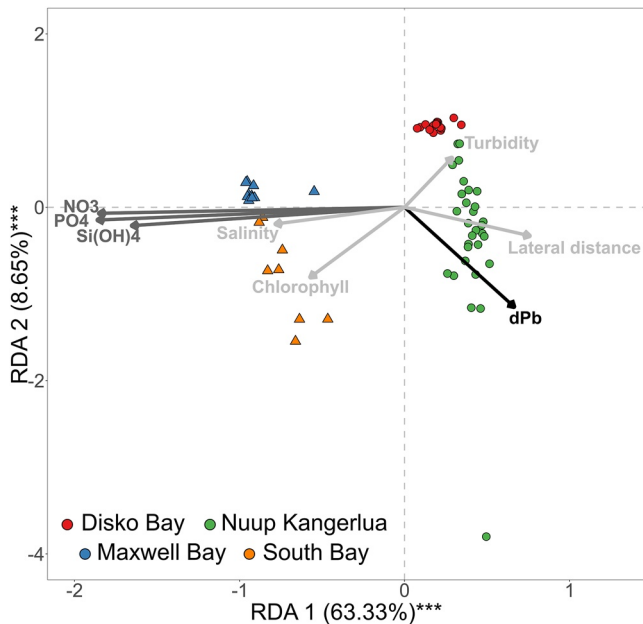


Figure 3. Redundancy analysis for dissolved lead (dPb) and other variables which may explain dPb dynamics. Only summertime data are plotted (austral summer January–February, boreal summer August–September).

The inner-fjord environments in all Arctic fjords herein are characterized by low photic zone depths (as low as 1–10 m, Murray et al., 2015), surface plumes of high turbidity and, in the innermost few kilometers of the fjord, typically high turbidity through the water column in summer (van Genuchten et al., 2021). It should be noted in discussing these trends, due to a combination of CTD and underway sampling there is no standardized measure of particle load across the data set, but spatial trends are consistent. In Ameralik, the highest turbidity loads were observed in the inner-fjord and then declined down fjord. High particle loads were visibly evident at the fjord surface and evidenced by extremely high concentrations of total dissolvable (soluble at pH 1.9) metals (e.g., 4.6–77 μM total dissolvable Fe at AM9 to AM12.5 in August 2019, Krause et al., 2021). In Disko Fjord, Qasigiannuguit and Kangaatsiaq turbidity was similarly elevated in the innermost fjord and then declined sharply moving down fjord (van Genuchten et al., 2021). In Nuup Kangerlua, a high particle load is evident in all available turbidity profiles in the inner-fjord close to the marine-terminating glacier Narsap Sermia (Hopwood et al., 2018) but, unlike Ameralik, is less of a sharp feature peaking in surface waters. Turbidity in Nuup Kangerlua then peaked again midfjord (close to GF11) due to outflow from a large lake (Tasersuaq) which receives discharge from land-terminating glaciers. This is reflected in midfjord peaks of many inorganic components including Si(OH)_4 , dFe, dNi, dCu, and dMn (Krause et al., 2021), but not dPb. The overall spatial pattern

of turbidity was an almost equally poor explaining factor for dPb distribution as salinity, although the RDA suggests opposite dynamics (Figure 3). Whereas dPb has almost no relationship with turbidity, it has a weak negative relationship with salinity (Figure 3).

CDOM S_R is a proxy for colored dissolved organic matter (DOM) molecular size, particularly for terrestrially derived humic substances (Helms et al., 2008), but is more complicated to interpret as it can reflect numerous changes to DOM. Microbial degradation tends to decrease S_R , photochemical bleaching tends to increase S_R , and an increasing fraction of CDOM of marine origin would also be expected to increase S_R (for marine CDOM $S_{275-295} > S_{350-400}$, whereas the opposite is the case for terrestrially derived CDOM (Helms et al., 2008). Across almost all transects S_R increased with increasing salinity, but the cause was variable reflecting changes in both $S_{350-400}$ and $S_{275-295}$. This implies a shift to dominance of marine-derived CDOM in higher salinity waters, which is consistent with autochthonous carbon fixation being a major organic carbon source to glacier fjord systems and terrestrial runoff being less significant at the fjord scale (Paulsen et al., 2017). Some contribution of photo-bleaching to trends in S_R occurring on the same timescale is plausible. The two notable exceptions were Ameralik in August 2019 and Nuup Kangerlua in September 2019. Based on a monthly time series of chl *a* and primary production measured at station GF3 in the mouth of Nuup Kangerlua (adjacent to Ameralik, Juul-Pedersen et al., 2015), and the high turbidity measured in Ameralik close to the peak of the runoff season, a reduced gradient in the change in S_R with salinity likely reflects both low in-fjord marine primary production and limited photo-bleaching at these times of year. In early September, productivity in Nuup Kangerlua has declined from its summertime peak (Juul-Pedersen et al., 2015; Meire et al., 2017). In Ameralik, the high turbidity within the fjord through summer (e.g., at 1 m depth for AM10 in 2019: 6.8 mg L⁻¹ in May, 16.0 mg L⁻¹ in August and 9.2 mg L⁻¹ in September, Stuart-Lee et al., 2023), combined with observations of residual nitrate in the inner-fjord (up to 1.5 μM), suggests a low-light, low-productivity environment where photochemical bleaching is limited and in-fjord formation of marine CDOM is also limited compared to the other glacier fjords discussed herein.

3.3. Incubation Experiments

The first incubation experiment revealed the sensitivity of dPb release from glacier-derived particles to particle loading. The highest dPb concentrations in solution were invariably associated with the highest particle loadings of ~500 mg L⁻¹ (Figure 4), but the most efficient release was from the lowest loadings of ~20 mg L⁻¹. The background concentration of dPb in the Atlantic water used for all incubations was consistently 16.2 ± 1.3 pM across all control treatments. In the first incubation with varying sediment load added to Atlantic water for 24 hr, dPb increased sharply from 16.2 pM as sediment load was increased up to 100 mg L⁻¹, but the increase in dPb was then less pronounced with sediment load increases up to 500 mg L⁻¹. Light and dark treatments were very similar for each sediment type. The only notable exceptions to this general trend were the two proglacial stream sediment samples (Figure 4). One of these showed a much more linear tendency for dPb to increase with sediment load, and both had a high increase in dPb concentration after 24 hr compared to other sediment (+17 pM and +148 pM, or release of 0.72 nmol g⁻¹ and 7.1 nmol g⁻¹, respectively). Particle sizes were very similar across the different particle types. For Kongsfjorden, the range (mean \pm standard deviation) particle size was 4.4–13 (7.8 ± 4.0 , $n = 7$) μm for glacier surface sediment, 7.5–14 (11 ± 2.3 , $n = 10$) μm for iceberg surface sediment, 3.4–15 (9.7 ± 4.7 , $n = 9$) μm for iceberg embedded sediment and 1.3–7.7 (3.2 ± 2.0 , $n = 10$) μm for proglacial stream flour.

The second incubation experiment, following dPb concentrations for up to 500 hr at sediment loadings of either 50 or 200 mg L⁻¹, suggested that the initial release of dPb over the first 24 hr is then followed by a decline in dPb concentrations toward a lower steady state concentration which is then sustained (Figure 5). The only exception to this observation was, again, a proglacial stream sediment sample which demonstrated increasing dPb over the first 200 hr. Across all incubations the difference between light and dark treatments was similar to what would be expected from random variation (mean concentrations comparing light/dark 1.00, median 0.99, standard deviation 0.25).

Sediment samples corresponding to the region where dPb data are available were iceberg-borne and suspended fjord particles collected from Nuup Kangerlua and Ameralik (SW Greenland). There are limited accessible proglacial sites where freshly released glacier-derived sediment can be obtained close to the large glaciers in Nuup Kangerlua, and so given the general hypothesis that glacier-derived particles may act as a dynamic source/sink for dPb we also conducted resuspension experiments using samples from Kongsfjorden (Svalbard) where

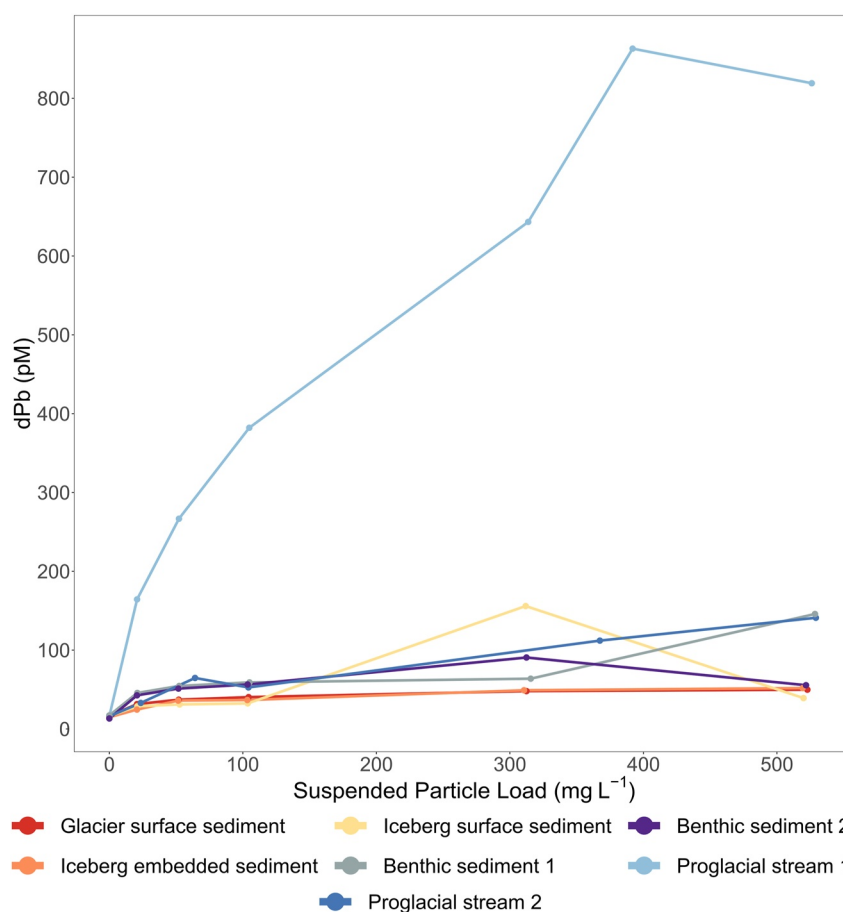


Figure 4. The observed dissolved lead (dPb) concentration with increasing suspended particle load contrasting different types of sediment/particles collected from Kongsfjorden (benthic sediments 1 and 2, glacier surface sediment, iceberg surface sediment, iceberg embedded sediment, proglacial streams 1 and 2, glacier surface sediment). No significant difference was detected between light and dark treatments for any experiment so plotted points are mean values of two replicate experiments (one light, one dark).

a much broader range of proglacial sedimentary environments can be sampled. Curiously, release of dPb from particles collected in Ameralik was extremely high compared to other sediment samples (dPb release of up to 20 nmol g^{-1} within 24 hr at 4°C). Release of dPb from particles collected in Ameralik appeared to be temperature sensitive, with consistently higher net release of dPb at higher temperatures (1.68 ± 0.22 -fold higher dPb concentrations at 11°C compared to 4°C). Dissolved Pb concentrations were still increasing after 8 days in suspension, which was also unusual relative to other sediments and similar only to some proglacial stream sediment from Kongsfjorden (Figure 5).

Labile Pb concentrations were determined on the particles used for incubations herein. Suspended particles in Ameralik fjord had a high LpPb content ($113 \pm 47 \text{ nmol g}^{-1}$) compared to other particles. The fraction of this Pb released as dPb in over 24 hr at 4°C was also relatively high (9%). While LpPb content was lower for two proglacial stream sediment samples from Kongsfjorden ($11\text{--}28 \text{ nmol g}^{-1}$), one of these also released a high fraction of Pb into seawater, equivalent to 26% of LpPb. All samples released the equivalent of $>2\%$ of LpPb into solution. It should be noted that the release of dPb was clearly sensitive to the sediment load, and thus some of the differences observed between different particle types may reflect small differences in particle load which varied slightly due to the use of wet slurry.

Total Pb concentrations for suspended particles in Kongsfjorden, after microwave digestion with HNO_3 and H_2O_2 , were previously reported to fall in the range $50\text{--}202 \text{ nmol g}^{-1}$ (Bazzano et al., 2017). No direct comparison of LpPb and total particulate Pb in the same samples is available, but if particle lability did not change over the timescale of particle additions to the fjord, the values herein are at least consistent and would suggest LpPb

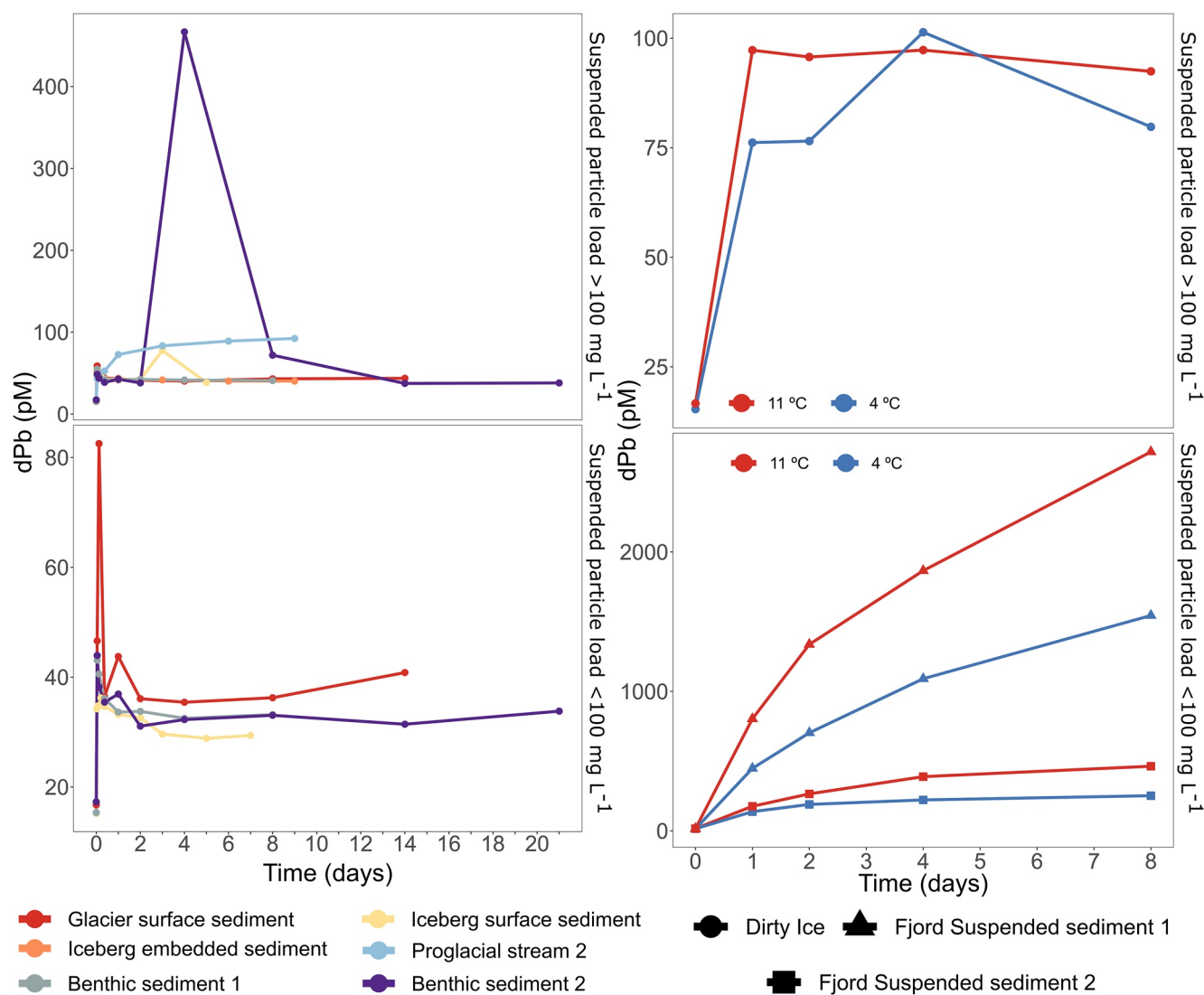


Figure 5. Observed dissolved lead (dPb) concentrations with increasing incubation time. (Left) Incubations were performed by adding sediment/particles collected from Kongsfjorden (benthic sediments 1 and 2, glacier surface sediment, iceberg surface sediment, iceberg embedded sediment, proglacial stream, glacier surface sediment) to seawater. No significant difference was detected between light and dark treatments for any experiment so plotted points are mean values of two replicate experiments. (Right) Incubations were performed by adding particles collected from SW Greenland: dirty ice particles from Nuup Kangerlua, fjord suspended particles from Ameralik.

accounts for roughly 5–60% of total Pb for Kongsfjorden particles. Near-surface (0–20 m) suspended particle loads in Ameralik and Nuup Kangerlua in September 2019 were $6.09 \pm 0.93 \text{ mg L}^{-1}$ and $5.30 \pm 0.38 \text{ mg L}^{-1}$, respectively (Stuart-Lee et al., 2023). Combined with a mean LpPb suspended particle content of 113 nmol g^{-1} measured in Ameralik (Table 1), LpPb is approximately present at a mean concentration of $\sim 0.7 \text{ nmol}$ in Ameralik.

4. Discussion

4.1. Comparison of dPb Distributions

When comparing dPb dynamics across the salinity gradient in Nuup Kangerlua with data from more temperate river estuaries (Annibaldi et al., 2015; Benoit et al., 1994; Guieu et al., 1996; Martin et al., 1993; Munksgaard & Parry, 2001; Wen et al., 1999), the spatial distribution of dPb is similar with the dPb concentrations falling at the low end of the range observed globally (Figure 6). The best fitting GAM depicted a specific salinity effect for each estuary (Figure 6) similar to the dynamics registered for glacial fjords (Figure 2). Similar to

Table 1
Labile Pb Content and Dissolved Pb Released From Glacier-Derived Particles in Seawater

| Particle type | Sediment origin | Details of prior work on sample | Labile Pb nmol g ⁻¹ | Released pmol g ⁻¹ (% of L _p Pb) ^a |
|---------------------------|-----------------|--|--------------------------------|--|
| Glacier surface sediment | Kongsfjorden | No. 13, Hopwood et al. (2017) | 18.0 | 720 (4.0%) |
| Iceberg surface sediment | Kongsfjorden | No. 78, Hopwood et al. (2017) | 28.1 | 598 (2.1%) |
| Iceberg embedded sediment | Kongsfjorden | No. 15, Hopwood et al. (2017) | 13.5 | 471 (3.5%) |
| Proglacial stream 1 | Kongsfjorden | No. 95, Hopwood et al. (2017) | 27.6 | 7,140 (25.9%) |
| Proglacial stream 2 | Kongsfjorden | No. 96, Hopwood et al. (2017) | 10.8 | 708 (6.6%) |
| Fjord suspended sediment | Ameralik | CTD1-3, van Genuchten et al. (2021) | 113 ± 47 (n = 3) | 20,300 (4°C, 18.0%) 51,800 (11°C, 45.8%) |
| Iceberg surface sediment | Nuup Kangerlua | n/a | 11.5 ± 1.4 (n = 5) | 279 (2.4%) ^b 457 (4.0%) ^c |
| Benthic, core-top 1 | Kongsfjorden | Core KF1, Laufer-Meiser et al. (2021) | n.d. | 1,450 (n.d.) |
| Benthic, core-top 2 | Kongsfjorden | Core KFa7, Laufer-Meiser et al. (2021) | n.d. | 1,350 (n.d.) |

Note. Duplicate sediment samples from Kongsfjorden and Ameralik were used in prior work to investigate the labile iron content of sediments (Hopwood et al., 2017; Laufer-Meiser et al., 2021; van Genuchten et al., 2021).

^aAll incubations refer to 24 hr. Sediment loads vary slightly due to the use of wet sediment slurry rather than freeze dried sediment, range for incubations (except where stated otherwise) is 15–24 mg L⁻¹. ^bSuspended sediment load 220 mg L⁻¹. ^cSuspended sediment load 176 mg L⁻¹. “n.d.” not determined.

the distribution of dPb within glacier fjords, there is no clear general trend across estuaries and whereas for some locations dPb increases with salinity, in others it diminishes (Figure 6). We exclude discussion of estuaries with extremely high freshwater dPb concentrations (e.g., the Nile and Galveston rivers, Abdel-Moati, 1990; Wen et al., 1999), where a general decrease of dPb with salinity is inevitably observed due to dilution of high freshwater dPb concentrations.

While dPb concentrations herein varied between catchments, when compared to other elements measured on the same transects (Fe, Co, Ni, Cu, and Mn) the dPb concentrations were notable for being not generally elevated at low salinities. For salinities >30, the mean dPb concentration is 32 ± 37 pM. Mean dPb concentrations at lower salinities were similar; 38 ± 57 pM for salinities <15, and 49 ± 45 pM for salinities 15.0–35.4 (Kruskal Wallis, chi-square = 4.76, *p* value = 0.03). Dissolved Pb concentrations in fjord/coastal seawater, excluding one outlier, ranged between 3 and 250 pM (median 33 pM). This is at least comparable to the 22 ± 4.3 pM at shelf stations in central E Greenland (cruise D354, Achterberg et al., 2020), 15 ± 3.5 pM at shelf stations in S Greenland (Zurbrick et al., 2018) and 6.2 ± 3.7 pM in NE Greenland (Krisch et al., 2022). Concentrations were also similar to the 46 pM reported for Cumberland Bay (South Georgia, Schlosser & Garbe-Schönberg, 2019), and 89 pM at the Amundsen Sea shelf break (Ndungu et al., 2016).

Considering the salinity range, dPb concentrations at lower salinities are consistent with freshwater dPb concentrations at the low end of the reported range for Greenland. This is expected because only a fraction of discharge arises from runoff originating from historical precipitation with the highest Pb content (c 1950–1980s, Boyle et al., 1994; Murozumi et al., 1969). At intermediate salinities however, the increased dPb concentrations in most catchments require a different explanation, as they appear too high to be explained by mixing between fresh and saline waters and clearly do not approximate the trend observed for other trace elements. We acknowledge that the broad range of Pb in fresh and fjord water precludes a robust assessment of dPb enrichment. Nevertheless, a similar process to that proposed in South Georgia, dissolution of labile Pb from glacier-derived particles (Schlosser & Garbe-Schönberg, 2019), seems likely to be leading to elevated dPb concentrations in fjord waters which are subsequently returned to particles—which may include biogenic particles. The intense sediment plumes in Greenland's fjords may therefore be a local source of dPb, although based on the low dPb concentrations along the East Greenland coastline (Achterberg et al., 2020; Zurbrick et al., 2018), it appears that much of this dPb is also then removed from surface waters within glacier fjords.

Incubation experiments support the hypothesis of a dynamic exchange of Pb suggesting a pronounced release of dPb occurs in the first day when glacier-derived particles are introduced into seawater, with the release of dPb highly dependent on sediment load, and to a lesser extent on temperature (Figures 4 and 5). The subsequent readsorption of dPb onto particle surfaces appears to result in quasi-steady state dPb concentration being established, in most cases, largely within 48 hr. The temporal dynamics of this process likely create difficulties in interpreting spatial trends in dPb for fjord transects discussed herein. Glacier-derived particles are released from numerous sources within each fjord including approximate point sources from runoff streams and the grounding lines of marine-terminating glaciers,

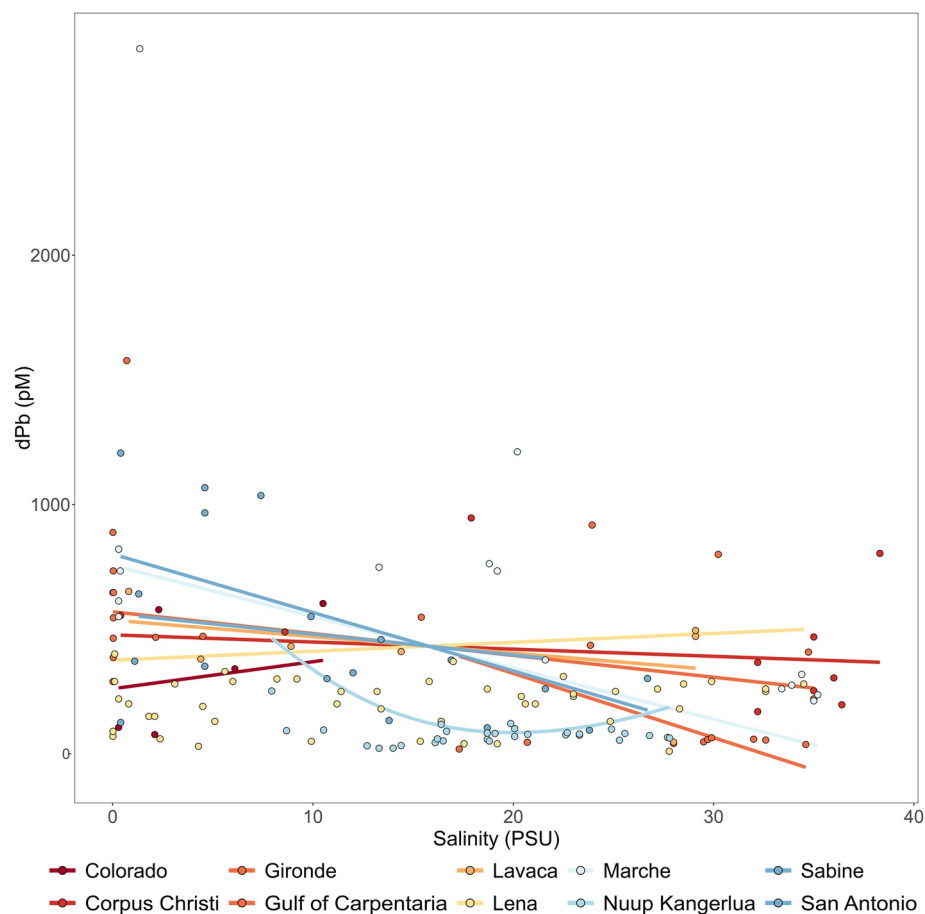


Figure 6. Concentrations of dissolved lead (dPb) across salinity gradients for riverine estuaries and a glacier fjord (Nuup Kangerlua). The best fitting GAM includes a salinity effect specific for each location. The distribution of dPb in Nuup Kangerlua (the best sampled site herein) is comparable to that observed in temperate estuaries though at the lower end of the range of observed concentrations.

but also from more diffuse sources such as iceberg melt and sediment resuspension. In addition to the formation of biogenic particles in more productive midfjord environments away from turbid plumes (Meire et al., 2017), this means turbidity is unlikely to show a simple, consistent relationship with dPb.

The higher dPb release from some proglacial stream sediment may reflect the progressive cycling of Pb between dissolved and particulate phases. Processing of sediment in proglacial environments is speculated to increase the labile fraction of several metals (Herbert et al., 2020). Both the incubation experiments and the nearshore high turbidity environments where runoff first enters the ocean are environments with minimal biogenic particle loads and so the major sink for dPb in these specific environments must be transfer to primarily lithogenic or authigenic particle phases. The high LpPb measured for some proglacial sediment and suspended fjord sediment samples may therefore have arisen from net adsorption of dPb in these high turbidity environments. The fraction of these particles that avoid sedimentation and are then diluted moving down fjord may then transition to a net source of dPb as sediment load declines and temperature (in surface waters) increases—both factors that seem to result in higher net dPb release. Two core-top sediments in Kongsfjorden, one from close to the glacier Kronebreen (KF1), and one from the fjord-mouth (KF7), both showed high dPb release compared to other sediment types (Table 1) which could reflect either trapping of labile Pb or increased lability in Pb from benthic processing within the fjord system. However, the broad range of dPb release from different sediment types even within the same fjord ($471\text{--}7,138\text{ mg L}^{-1}$ for Kongsfjorden, Table 1) precludes a conclusive comparison. Shifts in particle size should also be considered yet particle size changes alone are unlikely to explain the majority of differences between LpPb values as particle sizes for the Kongsfjorden glacier surface, iceberg surface and iceberg embedded samples were found to be similar (median particle sizes 8.2, 7.5, and 5.7 μm , respectively) thus varying less than LpPb content ($14\text{--}28\text{ nmol g}^{-1}$ for the same sediments, Table 1).

4.2. Seasonal Comparison of Nuup Kangerlua and Ameralik

It is important to note that while these two Greenlandic fjords are adjacent systems at a similar latitude, there are several distinct differences between them. Nuup Kangerlua is a much larger system both by area and volume with a surface area of 2,013 km², length of ~190 km and maximum depth of 620 m; compared to a 400 km² area, length of ~75 km and maximum depth of ~700 m for Ameralik (Mortensen et al., 2011, 2018; Stuart-Lee et al., 2021). While Ameralik receives summertime runoff only from a land-terminating glacier system at the fjord head, Nuup Kangerlua receives discharge from both marine-terminating and land-terminating systems which leads to significant differences in patterns of seasonal circulation and productivity (Juul-Pedersen et al., 2015; Stuart-Lee et al., 2021). A precise freshwater flux comparison is not possible due to different timescales and definitions within existing published work, but it is clear that Nuup Kangerlua experiences much larger inputs. For example, average 2002 to 2012 runoff in Nuup Kangerlua was estimated as 25.9 km³ yr⁻¹ (Langen et al., 2015) in addition to 7–10 km³ yr⁻¹ of calved ice (Van As et al., 2014). In contrast, 2012 runoff in Ameralik was estimated as 0.78 km³ yr⁻¹ (Overeem et al., 2015).

Specifically for 2019, physical oceanographic data for the same stations as studied herein shows that the onset of stratification was earlier in Ameralik, and stronger in July than in Nuup Kangerlua (Stuart-Lee et al., 2021). In later summer, this situation reversed and Nuup Kangerlua was more stratified (Stuart-Lee et al., 2021). While primary production measurements have not been published to date for Ameralik, productivity in Nuup Kangerlua is expected to be higher through summer due to enhanced vertical transport of macronutrients in Nuup Kangerlua from entrainment in marine-terminating glacier discharge plumes (Meire et al., 2017). In the absence of other confounding differences, higher productivity might be expected to increase the sink for dPb associated with incorporation into biogenic particles (Schlosser & Garbe-Schönberg, 2019), however summertime dPb concentrations were generally higher in Nuup Kangerlua. Furthermore, the largest difference in dPb concentrations was in spring, when dPb concentrations in Ameralik were much lower. These differences could relate to the exact timing of the cruise dates. In May 2019, chl *a* and fluorescence on the same cruise suggest higher biomass in Ameralik than in Nuup Kangerlua (Stuart-Lee et al., 2023). The cruise dates herein may therefore have been closer to the peak of the spring bloom in Ameralik. Thus the associated biological dPb sink may have also been relatively more important in Ameralik, particularly at the innermost stations. For example, contrasting AM9-AM12 with GF10-13 in May 2019, the Ameralik stations had chl *a* concentrations that were 3.4 fold higher, whereas suspended particle loads were similar along both fjords (6.29 ± 0.95 and 6.24 ± 0.61 mg L⁻¹ for the same Ameralik and Nuup Kangerlua stations).

A curious finding from GAM fittings was that dPb in Nuup Kangerlua positively correlated with chl *a* (Figure 2). This appears to run contrary to the expectation that plankton act as a major sink for dPb. However, this may relate to the temporal development of the phytoplankton bloom observed in this fjord with respect to the down fjord movement of freshwater and the associated dPb and particles. Close to glacier fronts chlorophyll concentrations are low due to a combination of estuarine circulation and the vertical entrainment of deep fjord water in a buoyant plume (Halbach et al., 2019; Meire et al., 2017). These processes ensure that water near the glacier fronts, where salinity is lowest and turbidity peaks, exhibit low chl *a* concentrations. Moving down fjord, turbidity declines and there is sufficient time for plankton biomass to increase as plankton grow in a stratified environment utilizing the supply of macronutrients from upwelled water. A bloom may therefore develop as is observed midfjord in Nuup Kangerlua (Meire et al., 2017). The position of the bloom, and thus a chl *a* maxima, coincides with the conditions favorable for efficient release of dPb (low turbidity and a warm stratified water column) and this may be what the positive relationship between dPb and chl *a* in a GAM (Figure 2) reflects.

4.3. Drivers of Estuarine dPb Trends

Temperate estuaries are far better studied field sites concerning the spatiotemporal variation in dPb dynamics. Lead is known to have a high affinity for adsorption onto particle surfaces (i.e., a high K_d value, Valenta et al., 1986), which decreases with particle load (Benoit et al., 1994). Estuarine dPb dynamics are therefore variable and depend on spatial/temporal changes in both particle load and redox state. In some cases dPb is reported to behave relatively conservatively in surface estuary transects or to show some evidence of net removal (Cenci & Martin, 2004; Françoise Elbaz-Poulichet et al., 1984; Wen et al., 1999). Yet there are many exceptions where dPb does not appear to show a clear trend over the salinity gradient, or can qualitatively be described as having a reasonably constant concentration over a broad range of salinities (Benoit et al., 1994; Windom et al., 1985).

Even when dPb concentrations are approximately constant, there may still be rapid exchange between dissolved and labile particulate phases and this has been explicitly confirmed in some estuarine waters where rapid isotopic exchange of Pb between these phases was found (Chen et al., 2016).

Deriving a meaningful “average” dPb trend for estuaries is inevitably a challenging exercise given the uneven distribution of studied sites with a bias toward northern Europe and North America, and the likelihood that the majority of sites reported in the literature have been strongly affected by historical anthropogenic Pb deposition. Both within estuaries and more generally across aquatic environments, scavenging of dPb onto particle surfaces is however a key feature of dPb distribution (Brügmann et al., 1985; Nozaki et al., 1997). Scavenging is driven both by cellular uptake or absorption onto cell walls, and by adsorption and coprecipitation of dPb onto Fe and Mn oxides (Nozaki et al., 1997; Windom et al., 1985). A high fraction of labile particulate Pb is bound to Fe/Mn oxides in some freshwater systems (Tessier et al., 1980) and dPb concentrations can thus be tightly coupled to dissolved Fe concentrations (Erel et al., 1991; Erel & Morgan, 1992). The precipitation or flocculation of Fe/Mn oxides, or their resuspension, can therefore be major drivers of dPb dynamics (Waeles et al., 2007; Wen et al., 1999). Suspended particle loads, Fe/Mn oxide dynamics and primary production are therefore key variables that may affect the rate of dPb transfer to particulate (including cellular) phases. All three of these factors show strong gradients in glacier fjords (Murray et al., 2015; van Genuchten et al., 2022; Zhang et al., 2015).

The correlation between dPb and most other elements considered herein was poor, both in the water column and in incubation experiments, with no element showing statistically significant correlation at the $p < 0.05$ level for both in situ and incubated conditions. The tendency of dPb to be scavenged on Fe oxide surfaces and released during Fe oxide dissolution might mean a correlation between dFe and dPb would be expected for in situ data (Waeles et al., 2007). However, dFe does not scale with particulate Fe concentrations and following rapid declines in dFe concentration at low salinities (Schroth et al., 2014; Zhang et al., 2015) is better described by relatively constant low nanomolar concentrations over the spatial scale of the glacier fjords considered herein (Krause et al., 2021; van Genuchten et al., 2021). That being the case, with a relatively constant concentration of 4–10 nM dFe across the salinity gradient in Arctic glacier fjords in summer despite total dissolvable Fe concentrations declining by a factor of 17–130 over the same spatial scale (Krause et al., 2021), a major role for particulate Fe in driving dPb removal would not lead to a correlation between dFe and dPb (Krause et al., 2021; van Genuchten et al., 2022).

4.4. Are Anthropogenic Pb Signals Evident?

The ranges of total dissolvable Pb reported around the Arctic vary, as determined after various acid digestions. For concentrations reported for ice or snow in Greenland, there is a broad range even when considering annual timescales (Boyle et al., 1994; Rosman et al., 1998). While there is certainly consensus that total dissolvable Pb concentrations in precipitation have increased since the industrial revolution and show a maxima in Greenland between the 1950s and 1980s (Boyle et al., 1994; Candelone et al., 1995; Hong et al., 1994), it is challenging to quantify the mean Pb concentration expected in runoff without high resolution regional data. Total dissolvable Pb concentrations range between ~2 and 800 pM in ice samples predating the industrial revolution (Cragin et al., 1975; Hong et al., 1994, 1996; Murozumi et al., 1969; Ng & Patterson, 1981), whereas the range for more recent ice/snow samples extends from 10 pM to low nanomolar concentrations (Boutron et al., 1993; Boyle et al., 1994; Candelone et al., 1995; Cragin et al., 1975; Davidson et al., 1981; Murozumi et al., 1969; Rosman et al., 1998). The ranges alone however are not directly comparable due to the higher resolution of more recent measurements and known strong seasonal variability in Pb deposition (Boyle et al., 1994).

Dissolved Pb trends herein do not show strong evidence of a direct freshwater-associated dPb source and it is clear that particle dynamics are a strong moderating influence on dPb concentrations across the salinity gradient. While no isotopic evidence is presented herein to robustly constrain the fraction of dPb arising from anthropogenic sources, the similarity of the concentrations and trends observed herein to those reported for other glaciated coastlines suggests a similar mechanism is operating. Primarily nonanthropogenic dPb released from glacier-derived particles, followed by readsorption onto particle surfaces or incorporation into new authigenic phases controls dPb availability. Glacier fjords and glaciated coastlines are therefore unusual environments in an Arctic and Atlantic context, as historical anthropogenic dPb deposition remains a major (Rusiecka et al., 2018; Schlosser & Garbe-Schönberg, 2019), although in most cases receding (Bridgestock et al., 2016), driver of dPb distributions in these regions more generally.

4.5. Implications for Pb Fluxes

Fluxes of nonconservative dissolved elements such as Fe and Pb are challenging to constrain across the land-ocean continuum because the derived flux from observational data is sensitive to the spatial scale, or fluxgate, used. In the case of Pb, this reflects the dynamic transfer of Pb between LpPb and dPb phases which has been invoked to explain dPb behavior in other marine shelf/coastal environments (Chen et al., 2016; Rusiecka et al., 2018; Schlosser & Garbe-Schönberg, 2019). Nevertheless, several different Pb fluxes can be derived from existing data which we discuss considering the caveats associated with each approach.

Precipitation and ice core Pb concentrations (for Greenland) have a very broad range from 2 to 800 pM suggesting that 1,200 km³ yr⁻¹ of freshwater discharge (Bamber et al., 2018) corresponds roughly to an annual release of between 2.4 and 960 kmol yr⁻¹ total Pb into the ocean. However, this approach ignores the potential role of subglacial and proglacial weathering as Pb sources (Hawkings et al., 2020; Krisch et al., 2022). At Leverett Glacier (west Greenland), a seasonal time series of dPb in runoff suggests a discharge weighted mean of 182 pM with a range from below detection to 666 pM (Hawkings et al., 2020). While similar to the range for ice/snow samples, which include higher values associated with anthropogenic pollution, the moderately high weighted mean may reflect a combination of a low contribution from ice melt overprinted with a contribution from subglacial weathering. Sediment incubations suggest a maximum dPb release from particles at low sediment loadings over short time periods (<24 hr) at warm temperatures. Under these conditions up to 46% of LpPb is released into solution. With total sediment fluxes of 0.91–1.29 Gton yr⁻¹ estimated for Greenland runoff and calved ice (Overeem et al., 2017), low/high LpPb content of 11.5/113 nmol g⁻¹, and low/high solubility of 2–46% (Table 1), the corresponding dPb fluxes are 0.22–67 Mmol yr⁻¹. The efficiency of this dPb release is however likely attenuated strongly by high sediment loads close to where the discharge of freshwater occurs. Only when a fraction of particles has been dispersed down fjord, with the suspended sediment load reduced through dilution and sedimentation, does dPb release likely approach the optimum conditions required for maximum dPb release. A lower estimate of dPb release could be deduced from using the percentage of LpPb released over longer time periods (>48 hr) at higher sediment loads. Under these circumstances, a relatively constant dPb concentration is found irrespective of sediment load (Figure 4) suggesting that dPb concentration approximates steady state and that the associated flux would therefore not scale with the total LpPb release from glaciers. The associated flux would instead depend on the volume of saline waters circulated through fjords as glacially modified waters, which to our knowledge has not been derived on a large, for example, pan-Greenland, scale.

One recent case study used excess helium, a tracer of glacial meltwater, to track dPb over the NE Greenland shelf and deduced a flux of 10.6 ± 6.8 kmol yr⁻¹ dPb emerging from the floating ice tongue of Nioghalvfjærdsbræ (Krisch et al., 2022). Nioghalvfjærdsbræ accounts for approximately 2% of the annual solid and liquid discharge from the Greenland Ice Sheet (Schaffer et al., 2020), so the magnitude of this local flux is at least consistent with the range deduced above. It is not possible to refine these calculations further without detailed depth profiles of Pb through the year to assess seasonal and spatial changes combined with a similar level of detail concerning suspended sediment dynamics and fjord overturning. The relationship between sediment discharge, runoff volume and turbidity is also unclear and may vary between catchments due to the confounding influence of watershed hydrology on the fate of suspended sediment (Chu et al., 2009, 2012; Normandeau et al., 2019). However, from these basic calculations and the observed dPb distribution it is clear that the dPb flux associated with runoff around Greenland is higher than can be explained by the total Pb content of ice indicating mobilization of dPb from proglacial or subglacial weathering (Hawkings et al., 2020). This is similar to the deductions that can be made from observed mercury (Hg) concentrations in the same Arctic environments. Melting of glacial ice is estimated to produce a total Hg flux of 0.40 ± 0.007 Mg yr⁻¹, whereas the total Hg flux associated with sedimentary export is estimated to be considerably larger, about 40 Mg yr⁻¹ (Dastoor et al., 2022). Thus, any dPb flux estimated from freshwater dPb concentrations, or atmospheric deposition on ice surfaces, will underestimate the dPb release into the marine environment.

In summary, the release of dPb from the present-day Greenland Ice Sheet into saline waters is likely within the range 0.2–1 Mmol yr⁻¹ but with considerable uncertainty concerning the effect of particle residence time in the water column on the release of dPb into seawater. Antarctic fluxes are much more challenging to derive given the paucity of the data and especially that both catchments considered herein receive discharge from only small ice caps, not the Antarctic Ice Sheet. For comparison to our derived Greenlandic flux range, recent estimates of Pb deposition over the Arctic are 0.08–5.96 nmol m⁻² day⁻¹ (summer 2015, western Arctic ocean,

Marsay et al., 2018) and $6.75 \pm 9.17 \text{ nmol m}^{-2} \text{ day}^{-1}$ (1990–1992, central Arctic, Kadko et al., 2016). Averaged across the area of the Arctic Ocean, this would equate to total Pb deposition of $0.41\text{--}30.6 \text{ Mmol yr}^{-1}$ and $24.6 \pm 47.0 \text{ Mmol yr}^{-1}$, respectively. The scales over which these fluxes are delivered obviously differs as runoff is more confined, so in regions receiving meltwater, the glacier-derived signal rather than atmospheric deposition is likely the major dPb source. This is consistent with prior work which has inferred locally dominant glacier-derived Pb sources in diverse regions worldwide (Colombo et al., 2019; Kim et al., 2015; Ndungu et al., 2016; Schlosser & Garbe-Schönberg, 2019).

5. Conclusions

Dissolved Pb distributions downstream of glaciers in the marine environment are markedly different from any other trace element for which data is available on the same spatial scale (dFe, dCo, dNi, dCu, dAl, and dMn). Release of dPb from glacier-derived particles creates an unusual dPb distribution which appears closer to constant concentrations across the salinity gradient than it does to a gradient toward higher or lower concentrations in saline waters. While unusual compared to other trace elements, this spatial distribution of dPb does resemble that observed in some lower latitude estuaries and is consistent with observations from incubation experiments. Around glaciated coastlines, dPb sources associated with glacier-derived particles are locally dominant over any anthropogenic influence, even though anthropogenic derived Pb is still a major influence on dPb distribution across the Atlantic as a whole (Bridgestock et al., 2016; Rusiecka et al., 2018).

Future trends in dPb in glacier catchments are challenging to predict as suspended sediment load is a strong moderating influence on the gross and net release of dPb, and increasing temperatures may also favor net dPb release. Present-day dPb release from the Greenland Ice Sheet is likely to be within the range $0.2\text{--}1 \text{ Mmol yr}^{-1}$, though the dynamic exchange of Pb between dissolved and particulate phases over short timescales (hours-days) means the magnitude of this flux is very sensitive to the spatial/temporal scale over which it is defined. In the context of Greenlandic glacier fjords temperatures warmer than $\sim 5^\circ\text{C}$ are unusual (Mascarenhas & Zielinski, 2019; Murray et al., 2015; Stuart-Lee et al., 2021) and only associated with strongly stratified summertime conditions which can result in a thin layer of warm, sometimes highly turbid surface waters. In other words, high temperatures are normally associated with strong stratification and thus inefficient dispersal of particles. Systematic shifts to higher dPb release at broad scales are therefore likely to be moderated by these counteracting effects. A temperature sensitivity of dPb release may however be particularly problematic for the proposed use of glacial flour as an agricultural or ocean alkalinity enhancement agent at lower latitudes (Gunnarsen et al., 2019) which could potentially increase the net dPb release into the environment.

Conflict of Interest

The authors declare no conflicts of interest relevant to this study.

Data Availability Statement

All biogeochemical data from transects are available from (Krause et al., 2021), a complete supplementary data file is also provided herein for ease of access. Incubation experiment data can be found via: Zhu et al. (2022), “LpPb and dPb dataset for ‘Glacier-derived particles as a regional control on marine dissolved Pb concentrations,’” Mendeley Data, V2, <https://doi.org/10.17632/rxzpf7453c.2>; and Zhu et al. (2023), “LPMe and dMe dataset for ‘Incubation experiments to characterize particle-dissolved trace metal dynamics in glacier plumes,’” Mendeley Data, V1, <https://doi.org/10.17632/ny5rt94vn2.1> (last accessed August 2023).

References

- Abdel-Moati, A. R. (1990). Behaviour and fluxes of copper and lead in the Nile River estuary. *Estuarine, Coastal and Shelf Science*, 30(2), 153–165. [https://doi.org/10.1016/0272-7714\(90\)90061-U](https://doi.org/10.1016/0272-7714(90)90061-U)
- Achterberg, E. P., Steigenberger, S., Klar, J. K., Browning, T. J., Marsay, C. M., Painter, S. C., et al. (2020). Trace element biogeochemistry in the high latitude North Atlantic ocean: Seasonal variations and volcanic inputs. *Global Biogeochemical Cycles*, 35, e2020GB006674. <https://doi.org/10.1029/2020GB006674>
- Annett, A. L., Skiba, M., Henley, S. F., Venables, H. J., Meredith, M. P., Statham, P. J., & Ganeshram, R. S. (2015). Comparative roles of upwelling and glacial iron sources in Ryder Bay, coastal western Antarctic Peninsula. *Marine Chemistry*, 176, 21–33. <https://doi.org/10.1016/j.marchem.2015.06.017>

Acknowledgments

Antarctic sampling was possible through FONDAP-IDEAL 15150003. Xunchi Zhu was funded by the Sino-German (CSC-DAAD) Postdoc Scholarship Program with HR-ICP-MS analysis funded by GEOMAR. Juan Höfer was supported by FONDECYT-Regular 1211338. Mark Hopwood received support from the DFG (Award HO 6321/1-1) and from the NSFC (RFIS-II 42150610482). Ship time and work in Nuup Kangerlua was conducted in collaboration with MarineBasis-Nuuk, part of the Greenland Ecosystem Monitoring project (GEM). We gratefully acknowledge contributions from the Danish Centre for Marine Research (DCH), Greenland Institute of Natural Resources (GINR) and the Instituto Antártico Chileno (INACH) for their logistical support. Tim Steffens (GEOMAR) is thanked for technical assistance with HR-ICP-MS. Thomas Juul-Pedersen (GINR), Te Liu and Katja Laufer-Meiser (GEOMAR) are thanked for assistance with sample collection. The captain and crew of RV Sanna and Escudero/Yelcho stations are thanked for providing field support. Stephan Krisch (Bundesanstalt für Gewässerkunde) is thanked for comments on the text.

- Annibaldi, A., Illuminati, S., Truzzi, C., Libani, G., & Scarponi, G. (2015). Pb, Cu and Cd distribution in five estuary systems of Marche, central Italy. *Marine Pollution Bulletin*, 96(1), 441–449. <https://doi.org/10.1016/j.marpolbul.2015.05.008>
- Azetsu-Scott, K., & Syvitski, J. P. M. (1999). Influence of melting icebergs on distribution, characteristics and transport of marine particles in an East Greenland fjord. *Journal of Geophysical Research*, 104(C3), 5321–5328. <https://doi.org/10.1029/1998JC900083>
- Bamber, J. L., Tedstone, A. J., King, M. D., Howat, I. M., Enderlin, E. M., van den Broeke, M. R., & Noel, B. (2018). Land ice freshwater budget of the Arctic and North Atlantic oceans: 1. Data, methods, and results. *Journal of Geophysical Research: Oceans*, 123, 1827–1837. <https://doi.org/10.1002/2017JC013605>
- Bazzano, A., Ardini, F., Terol, A., Rivaro, P., Soggia, F., & Grotti, M. (2017). Effects of the Atlantic water and glacial run-off on the spatial distribution of particulate trace elements in the Kongsfjorden. *Marine Chemistry*, 191, 16–23. <https://doi.org/10.1016/j.marchem.2017.02.007>
- Bendixen, M., Overeem, I., Rosing, M. T., Bjørk, A. A., Kjær, K. H., Kroon, A., et al. (2019). Promises and perils of sand exploitation in Greenland. *Nature Sustainability*, 2(2), 98–104. <https://doi.org/10.1038/s41893-018-0218-6>
- Bendtsen, J., Mortensen, J., Lennert, K., & Rysgaard, S. (2015). Heat sources for glacial ice melt in a West Greenland tidewater outlet glacier: The role of subglacial freshwater discharge. *Geophysical Research Letters*, 42, 4089–4095. <https://doi.org/10.1002/2015GL063846>
- Benoit, G., Oktay-Marshall, S. D., Cantu, A., Hood, E. M., Coleman, C. H., Corapcioglu, M. O., & Santschi, P. H. (1994). Partitioning of Cu, Pb, Ag, Zn, Fe, Al, and Mn between filter-retained particles, colloids, and solution in six Texas estuaries. *Marine Chemistry*, 45(4), 307–336. [https://doi.org/10.1016/0304-4203\(94\)90076-0](https://doi.org/10.1016/0304-4203(94)90076-0)
- Berger, C. J. M., Lippiatt, S. M., Lawrence, M. G., & Bruland, K. W. (2008). Application of a chemical leach technique for estimating labile particulate aluminum, iron, and manganese in the Columbia River plume and coastal waters off Oregon and Washington. *Journal of Geophysical Research*, 113, C00B01. <https://doi.org/10.1029/2007JC004703>
- Borcard, D., Gillet, F., & Legendre, P. (2011). *Numerical ecology with R*. Springer.
- Boutron, C. F., Ducroz, F. M., Görlach, U., Jaffrezo, J.-L., Davidson, C. I., & Bolshov, M. A. (1993). Variations in heavy metal concentrations in fresh Greenland snow from January to August 1989. *Atmospheric Environment, Part A: General Topics*, 27(17), 2773–2779. [https://doi.org/10.1016/0960-1686\(93\)90309-M](https://doi.org/10.1016/0960-1686(93)90309-M)
- Boyle, E. A., Sherrell, R. M., & Bacon, M. P. (1994). Lead variability in the western North Atlantic Ocean and central Greenland ice: Implications for the search for decadal trends in anthropogenic emissions. *Geochimica et Cosmochimica Acta*, 58(15), 3227–3238. [https://doi.org/10.1016/0016-7037\(94\)90050-7](https://doi.org/10.1016/0016-7037(94)90050-7)
- Bridgestock, L., van de Fliert, T., Rehkämper, M., Paul, M., Middag, R., Milne, A., et al. (2016). Return of naturally sourced Pb to Atlantic surface waters. *Nature Communications*, 7(1), 12921. <https://doi.org/10.1038/ncomms12921>
- Brown, M. T., Lippiatt, S. M., & Bruland, K. W. (2010). Dissolved aluminum, particulate aluminum, and silicic acid in northern Gulf of Alaska coastal waters: Glacial/riverine inputs and extreme reactivity. *Marine Chemistry*, 122(1–4), 160–175. <https://doi.org/10.1016/j.marchem.2010.04.002>
- Brügmann, L., Danielsson, L.-G., Magnusson, B., & Westerlund, S. (1985). Lead in the North sea and the North East Atlantic ocean. *Marine Chemistry*, 16(1), 47–60. [https://doi.org/10.1016/0304-4203\(85\)90027-1](https://doi.org/10.1016/0304-4203(85)90027-1)
- Candelone, J.-P., Hong, S., Pellone, C., & Boutron, C. F. (1995). Post-industrial revolution changes in large-scale atmospheric pollution of the northern hemisphere by heavy metals as documented in central Greenland snow and ice. *Journal of Geophysical Research*, 100(D8), 16605–16616. <https://doi.org/10.1029/95JD00989>
- Cauvy-François, S., & Dangles, O. (2019). A global synthesis of biodiversity responses to glacier retreat. *Nature Ecology and Evolution*, 3(12), 1675–1685. <https://doi.org/10.1038/s41559-019-1042-8>
- Cenci, R. M., & Martin, J.-M. (2004). Concentration and fate of trace metals in Mekong river Delta. *Science of the Total Environment*, 332(1), 167–182. <https://doi.org/10.1016/j.scitotenv.2004.01.018>
- Chen, M., Boyle, E. A., Lee, J.-M., Nurhati, I., Zurbrick, C., Switzer, A. D., & Carrasco, G. (2016). Lead isotope exchange between dissolved and fluvial particulate matter: A laboratory study from the Johor river estuary. *Philosophical Transactions of the Royal Society A: Mathematical, Physical & Engineering Sciences*, 374(2081), 20160054. <https://doi.org/10.1098/rsta.2016.0054>
- Chu, V. W., Smith, L. C., Rennermalm, A. K., Forster, R. R., & Box, J. E. (2012). Hydrologic controls on coastal suspended sediment plumes around the Greenland Ice Sheet. *The Cryosphere*, 6(1), 1–19. <https://doi.org/10.5194/tc-6-1-2012>
- Chu, V. W., Smith, L. C., Rennermalm, A. K., Forster, R. R., Box, J. E., & Reeh, N. (2009). Sediment plume response to surface melting and supraglacial lake drainages on the Greenland ice sheet. *Journal of Glaciology*, 55(194), 1072–1082. <https://doi.org/10.3189/002214309790794904>
- Colombo, M., Rogalla, B., Myers, P. G., Allen, S. E., & Orians, K. J. (2019). Tracing dissolved lead sources in the Canadian Arctic: Insights from the Canadian GEOTRACES Program. *ACS Earth and Space Chemistry*, 3(7), 1302–1314. <https://doi.org/10.1021/acsearthspacechem.9b00083>
- Cragin, J. H., Herron, M., & Langway, C. C. (1975). *The chemistry of 700 years of precipitation at Dye 3, Greenland*. Corps of Engineers, US Army Cold Regions Research and Engineering Laboratory.
- Crockett, K. C., Foster, G. L., Vance, D., Richards, D. A., & Tranter, M. (2013). A Pb isotope tracer of ocean-ice sheet interaction: The record from the NE Atlantic during the last glacial/interglacial cycle. *Quaternary Science Reviews*, 82, 133–144. <https://doi.org/10.1016/j.quascirev.2013.10.020>
- Dastoor, A., Angot, H., Bieser, J., Christensen, J. H., Douglas, T. A., Heimbürger-Boavida, L.-E., et al. (2022). Arctic mercury cycling. *Nature Reviews Earth & Environment*, 3(4), 270–286. <https://doi.org/10.1038/s43017-022-00269-w>
- Davidson, C. I., Chu, L., Grimm, T. C., Nasta, M. A., & Qamoos, M. P. (1981). Wet and dry deposition of trace elements onto the Greenland ice sheet. *Atmospheric Environment*, 15(8), 1429–1437. [https://doi.org/10.1016/0004-6981\(81\)90349-8](https://doi.org/10.1016/0004-6981(81)90349-8)
- Elbaz-Poullichet, F., Garnier, J. M., Guan, D. M., Martin, J. M., & Thomas, A. J. (1996). The conservative behaviour of trace metals (Cd, Cu, Ni and Pb) and as in the surface plume of stratified estuaries: Example of the Rhône river (France). *Estuarine, Coastal and Shelf Science*, 42(3), 289–310. <https://doi.org/10.1006/ECSS.1996.0021>
- Elbaz-Poullichet, F., Holliger, P., Wen Huang, W., & Martin, J.-M. (1984). Lead cycling in estuaries, illustrated by the Gironde estuary, France. *Nature*, 308(5958), 409–414. <https://doi.org/10.1038/308409a0>
- Erel, Y., & Morgan, J. J. (1992). The relationships between rock-derived lead and iron in natural waters. *Geochimica et Cosmochimica Acta*, 56(12), 4157–4167. [https://doi.org/10.1016/0016-7037\(92\)90258-K](https://doi.org/10.1016/0016-7037(92)90258-K)
- Erel, Y., Morgan, J. J., & Patterson, C. C. (1991). Natural levels of lead and cadmium in a remote mountain stream. *Geochimica et Cosmochimica Acta*, 55(3), 707–719. [https://doi.org/10.1016/0016-7037\(91\)90335-3](https://doi.org/10.1016/0016-7037(91)90335-3)
- Forsch, K. O., Hahn-Woernle, L., Sherrell, R. M., Rocanova, V. J., Bu, K., Burdige, D., et al. (2021). Seasonal dispersal of fjord meltwaters as an important source of iron and manganese to coastal Antarctic phytoplankton. *Biogeosciences*, 18(23), 6349–6375. <https://doi.org/10.5194/bg-18-6349-2021>
- Fortner, S. K., Mark, B. G., McKenzie, J. M., Bury, J., Trierweiler, A., Baraer, M., et al. (2011). Elevated stream trace and minor element concentrations in the foreland of receding tropical glaciers. *Applied Geochemistry*, 26(11), 1792–1801. <https://doi.org/10.1016/j.apgeochem.2011.06.003>

- Greenland Ecosystem Monitoring. The Greenland Ecosystem Monitoring (GEM) Database. Retrieved from <https://g-e-m.dk>
- Guiu, C., Huang, W. W., Martin, J. M., & Yong, Y. Y. (1996). Outflow of trace metals into the Laptev sea by the Lena river. *Marine Chemistry*, 53(3–4), 255–267. [https://doi.org/10.1016/0304-4203\(95\)00093-3](https://doi.org/10.1016/0304-4203(95)00093-3)
- Gunnarsen, K. C., Jensen, L. S., Gómez-Muñoz, B., Rosing, M. T., & de Neergaard, A. (2019). Glacially abraded rock flour from Greenland: Potential for macronutrient supply to plants. *Journal of Plant Nutrition and Soil Science*, 182(5), 846–856. <https://doi.org/10.1002/jpln.201800647>
- Halbach, L., Vihtakari, M., Duarte, P., Everett, A., Granskog, M. A., Hop, H., et al. (2019). Tidewater glaciers and bedrock characteristics control the phytoplankton growth environment in a fjord in the Arctic. *Frontiers in Marine Science*, 6. <https://doi.org/10.3389/fmars.2019.00254>
- Hansen, H. P., & Koroleff, F. (1999). Determination of nutrients. In K. Grasshoff, K. Kremling, & M. Ehrhardt (Eds.), *Methods of seawater analysis* (pp. 159–228). Wiley-VCH Verlag GmbH.
- Hastie, T., & Tibshirani, R. (2014). *Generalized additive Models*. Wiley StatsRef: Statistics Reference Online. <https://doi.org/10.1002/9781118445112.stat03141>
- Hawkings, J. R., Skidmore, M. L., Wadham, J. L., Priscu, J. C., Morton, P. L., Hatton, J. E., et al. (2020). Enhanced trace element mobilization by Earth's ice sheets. *Proceedings of the National Academy of Sciences of the United States of America*, 117(50), 31648–31659. <https://doi.org/10.1073/pnas.2014378117>
- Helms, J. R., Stubbins, A., Ritchie, J. D., Minor, E. C., Kieber, D. J., & Mopper, K. (2008). Absorption spectral slopes and slope ratios as indicators of molecular weight, source, and photobleaching of chromophoric dissolved organic matter. *Limnology and Oceanography*, 53(3), 955–969. <https://doi.org/10.4319/lo.2008.53.3.0955>
- Herbert, L. C., Riedinger, N., Michaud, A. B., Laufer, K., Røy, H., Jørgensen, B. B., et al. (2020). Glacial controls on redox-sensitive trace element cycling in Arctic fjord sediments (Spitsbergen, Svalbard). *Geochimica et Cosmochimica Acta*, 271, 33–60. <https://doi.org/10.1016/j.gca.2019.12.005>
- Hong, S., Candelone, J.-P., Patterson, C. C., & Boutron, C. F. (1994). Greenland ice evidence of hemispheric lead pollution two millennia ago by Greek and Roman civilizations. *Science*, 265(5180), 1841–1843. <https://doi.org/10.1126/science.265.5180.1841>
- Hong, S., Candelone, J.-P., Turetta, C., & Boutron, C. F. (1996). Changes in natural lead, copper, zinc and cadmium concentrations in central Greenland ice from 8250 to 149,100 years ago: Their association with climatic changes and resultant variations of dominant source contributions. *Earth and Planetary Science Letters*, 143(1), 233–244. [https://doi.org/10.1016/0012-821X\(96\)00137-9](https://doi.org/10.1016/0012-821X(96)00137-9)
- Hopwood, M. J., Cantoni, C., Clarke, J. S., Cozzi, S., & Achterberg, E. P. (2017). The heterogeneous nature of Fe delivery from melting icebergs. *Geochemical Perspectives Letters*, 3(2), 200–209. <https://doi.org/10.7185/geochemlet.1723>
- Hopwood, M. J., Carroll, D., Browning, T. J., Meire, L., Mortensen, J., Krisch, S., & Achterberg, E. P. (2018). Non-linear response of summertime marine productivity to increased meltwater discharge around Greenland. *Nature Communications*, 9(1), 3256. <https://doi.org/10.1038/s41467-018-05488-8>
- IPCC Working Groups I & II. (2019). *Special report on the ocean and cryosphere in a changing climate (SROCC)*. Intergovernmental Panel on Climate.
- Juul-Pedersen, T., Arendt, K. E., Mortensen, J., Blicher, M. E., Sjøgaard, D., & Rysgaard, S. (2015). Seasonal and interannual phytoplankton production in a sub-Arctic tidewater outlet glacier fjord, SW Greenland. *Marine Ecology Progress Series*, 524, 27–38. <https://doi.org/10.3354/meps11174>
- Kadko, D., Galfond, B., Landing, W. M., & Shelley, R. U. (2016). Determining the pathways, fate, and flux of atmospherically derived trace elements in the Arctic ocean/ice system. *Marine Chemistry*, 182, 38–50. <https://doi.org/10.1016/j.marchem.2016.04.006>
- Kanna, N., Sugiyama, S., Fukamachi, Y., Nomura, D., & Nishioka, J. (2020). Iron supply by subglacial discharge into a fjord near the front of a marine-terminating glacier in Northwestern Greenland. *Global Biogeochemical Cycles*, 34, e2020GB006567. <https://doi.org/10.1029/2020GB006567>
- Kim, I., Kim, G., & Choy, E. J. (2015). The significant inputs of trace elements and rare earth elements from melting glaciers in Antarctic coastal waters. *Polar Research*, 34(1), 24289. <https://doi.org/10.3402/polar.v34.24289>
- Krause, J., Hopwood, M. J., Höfer, J., Krisch, S., Achterberg, E. P., Alarcón, E., et al. (2021). Trace element (Fe, Co, Ni and Cu) dynamics across the salinity gradient in Arctic and Antarctic glacier fjords. *Frontiers in Earth Science*, 9, 878. <https://doi.org/10.3389/feart.2021.725279>
- Krisch, S., Hopwood, M. J., Schaffer, J., Al-Hashem, A., Höfer, J., Rutgers van der Loeff, M. M., et al. (2021). The 79°N Glacier cavity modulates subglacial iron export to the NE Greenland Shelf. *Nature Communications*, 12(1), 3030. <https://doi.org/10.1038/s41467-021-23093-0>
- Krisch, S., Huhn, O., Al-Hashem, A., Hopwood, M. J., Lodeiro, P., & Achterberg, E. P. (2022). Quantifying ice-sheet derived lead (Pb) fluxes to the ocean; A case study at Nioghalvfjærdbræ. *Geophysical Research Letters*, 49, e2022GL100296. <https://doi.org/10.1029/2022GL100296>
- Langen, P. L., Mottram, R. H., Christensen, J. H., Boberg, F., Rodehacke, C. B., Stendel, M., et al. (2015). Quantifying Energy and mass fluxes controlling Godthåbsfjord freshwater input in a 5-km Simulation (1991–2012). *Journal of Climate*, 28(9), 3694–3713. <https://doi.org/10.1175/JCLI-D-14-00271.1>
- Laufer-Meiser, K., Michaud, A. B., Maisch, M., Byrne, J. M., Kappler, A., Patterson, M. O., et al. (2021). Potentially bioavailable iron produced through benthic cycling in glaciated Arctic fjords of Svalbard. *Nature Communications*, 12(1), 1349. <https://doi.org/10.1038/s41467-021-21558-w>
- Lokas, E., Zaborska, A., Kolicka, M., Różycki, M., & Zawierucha, K. (2016). Accumulation of atmospheric radionuclides and heavy metals in cryoconite holes on an Arctic glacier. *Chemosphere*, 160, 162–172. <https://doi.org/10.1016/j.chemosphere.2016.06.051>
- Mankoff, K. D., Noël, B., Fettweis, X., Ahlstrøm, A. P., Colgan, W., Kondo, K., et al. (2020). Greenland liquid water discharge from 1958 through 2019. *Earth System Science Data*, 12(4), 2811–2841. <https://doi.org/10.5194/essd-12-2811-2020>
- Mankoff, K. D., Solgaard, A., Colgan, W., Ahlstrøm, A. P., Khan, S. A., & Fausto, R. S. (2020). Greenland Ice Sheet solid ice discharge from 1986 through March 2020. *Earth System Science Data*, 12(2), 1367–1383. <https://doi.org/10.5194/essd-12-1367-2020>
- Marsay, C. M., Kadko, D., Landing, W. M., Morton, P. L., Summers, B. A., & Buck, C. S. (2018). Concentrations, provenance and flux of aerosol trace elements during US GEOTRACES Western Arctic cruise GN01. *Chemical Geology*, 502, 1–14. <https://doi.org/10.1016/j.chemgeo.2018.06.007>
- Martin, J. M., Guan, D. M., Elbaz-Poulichet, F., Thomas, A. J., & Gordeev, V. V. (1993). Preliminary assessment of the distributions of some trace elements (As, Cd, Cu, Fe, Ni, Pb and Zn) in a pristine aquatic environment: The Lena River estuary (Russia). *Marine Chemistry*, 43(1), 185–199. [https://doi.org/10.1016/0304-4203\(93\)90224-C](https://doi.org/10.1016/0304-4203(93)90224-C)
- Mascarenhas, V. J., & Zielinski, O. (2019). Hydrography-driven optical domains in the Vaigat-Disko bay and Godthåbsfjord: Effects of glacial meltwater discharge. *Frontiers in Marine Science*, 6. <https://doi.org/10.3389/fmars.2019.00335>
- Meire, L., Meire, P., Struyf, E., Krawczyk, D. W., Arendt, K. E., Yde, J. C., et al. (2016). High export of dissolved silica from the Greenland Ice Sheet. *Geophysical Research Letters*, 43(17), 9173–9182. <https://doi.org/10.1002/2016GL070191>
- Meire, L., Mortensen, J., Meire, P., Juul-Pedersen, T., Sejr, M. K., Rysgaard, S., et al. (2017). Marine-terminating glaciers sustain high productivity in Greenland fjords. *Global Change Biology*, 23(12), 5344–5357. <https://doi.org/10.1111/gcb.13801>

- Merwe, P. V. D., Wuttig, K., Holmes, T., Trull, T. W., Chase, Z., Townsend, A. T., et al. (2019). High lability Fe particles sourced from glacial erosion can meet previously unaccounted biological demand: Heard Island, southern ocean. *Frontiers in Marine Science*, *6*(332), 1–20. <https://doi.org/10.3389/fmars.2019.00332>
- Michael, S. M., Crusius, J., Schroth, A. W., Campbell, R., & Resing, J. A. (2023). Glacial meltwater and sediment resuspension can be important sources of dissolved and total dissolvable aluminum and manganese to coastal ocean surface waters. *Limnology & Oceanography*, *68*(6), 1201–1215. <https://doi.org/10.1002/lno.12339>
- Michaels, A. F., & Flegal, A. R. (1990). Lead in marine planktonic organisms and pelagic food webs. *Limnology & Oceanography*, *35*(2), 287–295. <https://doi.org/10.4319/lno.1990.35.2.0287>
- Mortensen, J., Bendtsen, J., Motyka, R. J., Lennert, K., Truffer, M., Fahnestock, M., & Rysgaard, S. (2013). On the seasonal freshwater stratification in the proximity of fast-flowing tidewater outlet glaciers in a sub-Arctic sill fjord. *Journal of Geophysical Research-Oceans*, *118*, 1382–1395. <https://doi.org/10.1002/jgrc.20134>
- Mortensen, J., Lennert, K., Bendtsen, J., & Rysgaard, S. (2011). Heat sources for glacial melt in a sub-Arctic fjord (Godthabsfjord) in contact with the Greenland Ice Sheet. *Journal of Geophysical Research*, *116*, C01013. <https://doi.org/10.1029/2010JC006528>
- Mortensen, J., Rysgaard, S., Arendt, K. E., Juul-Pedersen, T., Søgaard, D. H., Bendtsen, J., & Meire, L. (2018). Local coastal water masses control heat levels in a west Greenland tidewater outlet glacier fjord. *Journal of Geophysical Research: Oceans*, *123*, 8068–8083. <https://doi.org/10.1029/2018JC014549>
- Munksgaard, N. C., & Parry, D. L. (2001). Trace metals, arsenic and lead isotopes in dissolved and particulate phases of North Australian coastal and estuarine seawater. *Marine Chemistry*, *75*(3), 165–184. [https://doi.org/10.1016/S0304-4203\(01\)00033-0](https://doi.org/10.1016/S0304-4203(01)00033-0)
- Murozumi, M., Chow, T. J., & Patterson, C. (1969). Chemical concentrations of pollutant lead aerosols, terrestrial dusts and sea salts in Greenland and Antarctic snow strata. *Geochimica et Cosmochimica Acta*, *33*(10), 1247–1294. [https://doi.org/10.1016/0016-7037\(69\)90045-3](https://doi.org/10.1016/0016-7037(69)90045-3)
- Murray, C., Markager, S., Stedmon, C. A., Juul-Pedersen, T., Sejir, M. K., & Bruhn, A. (2015). The influence of glacial melt water on bio-optical properties in two contrasting Greenlandic fjords. *Estuarine, Coastal and Shelf Science*, *163*(PB), 72–83. <https://doi.org/10.1016/j.ecss.2015.05.041>
- Ndungu, K., Zurbrick, C. M., Stammerjohn, S., Severmann, S., Sherrell, R. M., & Flegal, A. R. (2016). Lead sources to the Amundsen Sea, west Antarctica. *Environmental Science & Technology*, *50*(12), 6233–6239. <https://doi.org/10.1021/acs.est.5b05151>
- Ng, A., & Patterson, C. (1981). Natural concentrations of lead in ancient Arctic and Antarctic ice. *Geochimica et Cosmochimica Acta*, *45*(11), 2109–2121. [https://doi.org/10.1016/0016-7037\(81\)90064-8](https://doi.org/10.1016/0016-7037(81)90064-8)
- Noble, A. E., Echegoyen-Sanz, Y., Boyle, E. A., Ohnemus, D. C., Lam, P. J., Kayser, R., et al. (2015). Dynamic variability of dissolved Pb and Pb isotope composition from the U.S. North Atlantic GEOTRACES transect. *Deep Sea Research Part II: Topical Studies in Oceanography*, *116*, 208–225. <https://doi.org/10.1016/j.dsr2.2014.11.011>
- Normandeau, A., Dietrich, P., Hughes Clarke, J., Van Wychen, W., Lajeunesse, P., Burgess, D., & Ghienne, J.-F. (2019). Retreat pattern of glaciers controls the occurrence of turbidity currents on high-latitude fjord Deltas (Eastern Baffin Island). *Journal of Geophysical Research: Earth Surface*, *124*(6), 1559–1571. <https://doi.org/10.1029/2018JF004970>
- Nozaki, Y., Zhang, J., & Takeda, A. (1997). ²¹⁰Pb and ²¹⁰Po in the equatorial Pacific and the Bering sea: The effects of biological productivity and boundary scavenging. *Deep Sea Research Part II: Topical Studies in Oceanography*, *44*(9), 2203–2220. [https://doi.org/10.1016/S0967-0645\(97\)00024-6](https://doi.org/10.1016/S0967-0645(97)00024-6)
- Oksanen, J., Blanchet, F. G., Friendly, M., Kindt, R., Legendre, P., McGlenn, D., et al. (2020). vegan: Community Ecology package.
- Overeem, I., Hudson, B., Welty, E., Mikkelsen, A., Bamber, J., Petersen, D., et al. (2015). River inundation suggests ice-sheet runoff retention. *Journal of Glaciology*, *61*(228), 776–788. <https://doi.org/10.3189/2015JG015102>
- Overeem, I., Hudson, B. D., Syvitski, J. P. M., Mikkelsen, A. B., Hasholt, B., van den Broeke, M. R., et al. (2017). Substantial export of suspended sediment to the global oceans from glacial erosion in Greenland. *Nature Geoscience*, *10*(11), 859–863. <https://doi.org/10.1038/ngeo3046>
- Paulsen, M. L., Nielsen, S. E. B., Müller, O., Møller, E. F., Stedmon, C. A., Juul-Pedersen, T., et al. (2017). Carbon bioavailability in a high Arctic fjord influenced by glacial meltwater, NE Greenland. *Frontiers in Marine Science*, *4*, 176. <https://doi.org/10.3389/fmars.2017.00176>
- Pesch, C., Weber, P. L., Moldrup, P., de Jonge, L. W., Arthur, E., & Greve, M. H. (2021). Physical characterization of glacial rock flours from fjord deposits in South Greenland—Toward soil amendment. *Soil Science Society of America Journal*, *86*(2), 407–422. <https://doi.org/10.1002/saj2.20352>
- Raiswell, R., Vu, H. P., Brinza, L., & Benning, L. G. (2010). The determination of labile Fe in ferrihydrite by ascorbic acid extraction: Methodology, dissolution kinetics and loss of solubility with age and de-watering. *Chemical Geology*, *278*(1–2), 70–79. <https://doi.org/10.1016/j.chemgeo.2010.09.002>
- Rapp, I., Schlosser, C., Rusiecka, D., Gledhill, M., & Achterberg, E. P. (2017). Automated preconcentration of Fe, Zn, Cu, Ni, Cd, Pb, Co, and Mn in seawater with analysis using high-resolution sector field inductively-coupled plasma mass spectrometry. *Analytica Chimica Acta*, *976*, 1–13. <https://doi.org/10.1016/j.aca.2017.05.008>
- R Core Team. (2012). *R: A Language and environment for statistical Computing*. R Foundation for Statistical Computing.
- Rosman, K. J. R., Chisholm, W., Boutron, C. F., Candelone, J.-P., Jaffrezo, J.-L., & Davidson, C. I. (1998). Seasonal variations in the origin of lead in snow at Dye 3, Greenland. *Earth and Planetary Science Letters*, *160*(3), 383–389. [https://doi.org/10.1016/S0012-821X\(98\)00098-3](https://doi.org/10.1016/S0012-821X(98)00098-3)
- Rusiecka, D., Gledhill, M., Milne, A., Achterberg, E. P., Annett, A. L., Atkinson, S., et al. (2018). Anthropogenic signatures of lead in the North-east Atlantic. *Geophysical Research Letters*, *45*, 2734–2743. <https://doi.org/10.1002/2017GL076825>
- Schaffer, J., Kanzow, T., von Appen, W. J., Appen, W.-J., von Albedyll, L., Arndt, J. E., & Roberts, D. H. (2020). Bathymetry constrains ocean heat supply to Greenland's largest glacier tongue. *Nature Geoscience*, *13*(3), 227–231. <https://doi.org/10.1038/s41561-019-0529-x>
- Schlosser, C., & Garbe-Schönberg, D. (2019). Mechanisms of Pb supply and removal in two remote (sub-)polar ocean regions. *Marine Pollution Bulletin*, *149*, 110659. <https://doi.org/10.1016/j.marpolbul.2019.110659>
- Schlosser, C., Schmidt, K., Aquilina, A., Homoky, W. B., Castrillejo, M., Mills, R. A., et al. (2018). Mechanisms of dissolved and labile particulate iron supply to shelf waters and phytoplankton blooms off South Georgia, Southern Ocean. *Biogeosciences*, *15*(16), 4973–4993. <https://doi.org/10.5194/bg-15-4973-2018>
- Schroth, A. W., Crusius, J., Campbell, R. W., & Hoyer, I. (2014). Estuarine removal of glacial iron and implications for iron fluxes to the ocean. *Geophysical Research Letters*, *41*, 3951–3958. <https://doi.org/10.1002/2014GL060199>
- Shaw, T. J., Raiswell, R., Hexel, C. R., Vu, H. P., Moore, W. S., Dudgeon, R., & Smith, K. L., Jr. (2011). Input, composition, and potential impact of terrigenous material from free-drifting icebergs in the Weddell Sea. *Deep-Sea Research Part II: Topical Studies in Oceanography*, *58*(11–12), 1376–1383. <https://doi.org/10.1016/j.dsr2.2010.11.012>
- Sherrell, R. M., Boyle, E. A., & Hamelin, B. (1992). Isotopic equilibration between dissolved and suspended particulate lead in the Atlantic Ocean: Evidence from ²¹⁰Pb and stable Pb isotopes. *Journal of Geophysical Research*, *97*(C7), 11257–11268. <https://doi.org/10.1029/92JC00759>

- Stuart-Lee, A. E., Mortensen, J., Juul-Pedersen, T., Middelburg, J. J., Soetaert, K., Hopwood, M. J., et al. (2023). Influence of glacier type on bloom phenology in two Southwest Greenland fjords. *Estuarine, Coastal and Shelf Science*, 284, 108271. <https://doi.org/10.1016/j.ecss.2023.108271>
- Stuart-Lee, A. E., Mortensen, J., van der Kaaden, A.-S., & Meire, L. (2021). Seasonal hydrography of Ameralik: A southwest Greenland fjord impacted by a land-terminating glacier. *Journal of Geophysical Research: Oceans*, 126, e2021JC017552. <https://doi.org/10.1029/2021JC017552>
- Tessier, A., Campbell, P. G. C., & Bisson, M. (1980). Trace metal speciation in the Yamaska and St. François rivers (Quebec). *Canadian Journal of Earth Sciences*, 17(1), 90–105. <https://doi.org/10.1139/e80-008>
- Valenta, P., Duursma, E. K., Merks, A. G. A., Rützel, H., & Nürnberg, H. W. (1986). Distribution of Cd, Pb and Cu between the dissolved and particulate phase in the Eastern Scheldt and western Scheldt estuary. *Science of The Total Environment*, 53(1), 41–76. [https://doi.org/10.1016/0048-9697\(86\)90092-6](https://doi.org/10.1016/0048-9697(86)90092-6)
- Van As, D., Andersen, M. L., Petersen, D., Fettweis, X., Van Angelen, J. H., Lenaerts, J. T. M., et al. (2014). Increasing meltwater discharge from the Nuuk region of the Greenland ice sheet and implications for mass balance (1960–2012). *Journal of Glaciology*, 60(220), 314–322. <https://doi.org/10.3189/2014JG0G13J065>
- van Genuchten, C. M., Hopwood, M. J., Liu, T., Krause, J., Achterberg, E. P., Rosing, M. T., & Meire, L. (2022). Solid-phase Mn speciation in suspended particles along meltwater-influenced fjords of West Greenland. *Geochimica et Cosmochimica Acta*, 326, 180–198. <https://doi.org/10.1016/j.gca.2022.04.003>
- van Genuchten, C. M., Rosing, M. T., Hopwood, M. J., Liu, T., Krause, J., & Meire, L. (2021). Decoupling of particles and dissolved iron downstream of Greenlandic glacier outflows. *Earth and Planetary Science Letters*, 576, 117234. <https://doi.org/10.1016/j.epsl.2021.117234>
- Waeles, M., Riso, R. D., & Le Corre, P. (2007). Distribution and seasonal changes of lead in an estuarine system affected by agricultural practices: The Penzé estuary, NW France. *Estuarine, Coastal and Shelf Science*, 74(3), 570–578. <https://doi.org/10.1016/j.ecss.2007.05.002>
- Wen, L.-S., Santschi, P., Gill, G., & Paternostro, C. (1999). Estuarine trace metal distributions in Galveston bay: Importance of colloidal forms in the speciation of the dissolved phase. *Marine Chemistry*, 63(3), 185–212. [https://doi.org/10.1016/S0304-4203\(98\)00062-0](https://doi.org/10.1016/S0304-4203(98)00062-0)
- Windom, H. L., Smith, R. G., & Maeda, M. (1985). The geochemistry of lead in rivers, estuaries and the continental shelf of the Southeastern United States. *Marine Chemistry*, 17(1), 43–56. [https://doi.org/10.1016/0304-4203\(85\)90035-0](https://doi.org/10.1016/0304-4203(85)90035-0)
- Wood, S. N. (2011). Fast stable restricted maximum likelihood and marginal likelihood estimation of semiparametric generalized linear models. *Journal of the Royal Statistical Society: Series B*, 73(1), 3–36. <https://doi.org/10.1111/j.1467-9868.2010.00749.x>
- Zhang, R., John, S. G., Zhang, J., Ren, J., Wu, Y., Zhu, Z., et al. (2015). Transport and reaction of iron and iron stable isotopes in glacial meltwaters on Svalbard near Kongsfjorden: From rivers to estuary to ocean. *Earth and Planetary Science Letters*, 424, 201–211. <https://doi.org/10.1016/j.epsl.2015.05.031>
- Zhu, X., Hopwood, M., & Achterberg, E. (2022). LpPb and dPb dataset for 'Glacier-derived particles as a regional control on marine dissolved Pb concentrations'. [Dataset]. Mendeley DataV2. <https://doi.org/10.17632/rxzf7453c.2>
- Zhu, X., Hopwood, M., & Achterberg, E. (2023). LPMe and dMe dataset for 'Incubation experiments to characterize particle-dissolved trace metal dynamics in glacier plumes'. [Dataset]. Mendeley DataV2. <https://doi.org/10.17632/ny5rt94vn2.1>
- Zurbrugg, C. M., Boyle, E. A., Kayser, R. J., Reuer, M. K., Wu, J., Planquette, H., et al. (2018). Dissolved Pb and Pb isotopes in the North Atlantic from the GEOVIDE transect (GEOTRACES GA-01) and their decadal evolution. *Biogeosciences*, 15(16), 4995–5014. <https://doi.org/10.5194/bg-15-4995-2018>